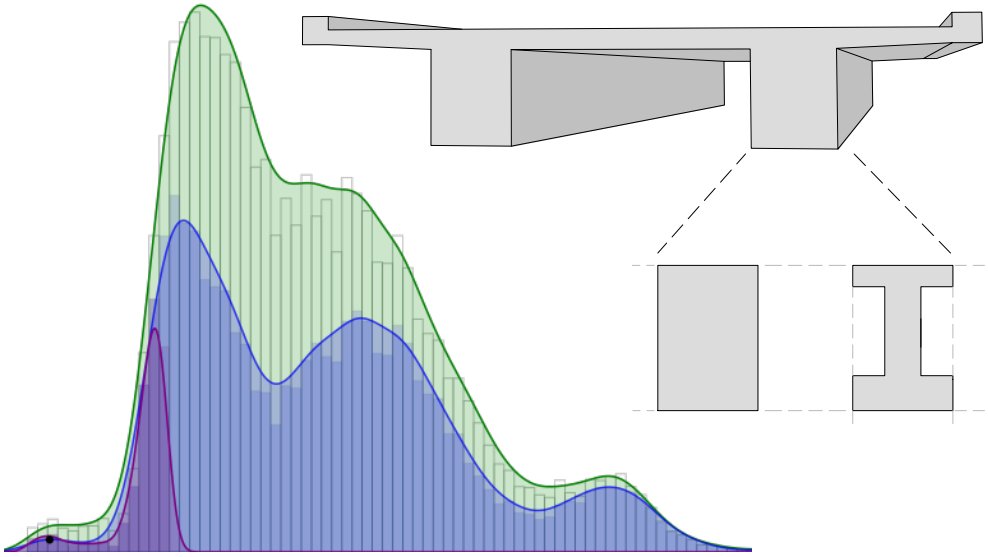

Early-Stage Design of Concrete Girder Bridges Using Set-Based Design

Parametric Exploration of Design Alternatives Considering CO_2 Emissions, Cost, and Buildability

Master's thesis in Structural Engineering and Building Technology

ALICE BEISCHER
KARIN FURUHJELM

DEPARTMENT OF ARCHITECTURE AND CIVIL ENGINEERING
DEVISION OF STRUCTURAL ENGINEERING

CHALMERS UNIVERSITY OF TECHNOLOGY
Master's thesis ACEX30
Gothenburg, Sweden 2025

MASTER'S THESIS ACEX30

Early-Stage Design of Concrete Girder Bridges Using Set-Based Design

Parametric Exploration of Design Alternatives Considering CO_2 Emissions, Cost, and Buildability

Master's Thesis in the Master's Programme Structural Engineering and Building Technology

ALICE BEISCHER
KARIN FURUHJELM

Department of Architecture and Civil Engineering
Division of Structural Engineering
CHALMERS UNIVERSITY OF TECHNOLOGY
Gothenburg, Sweden 2025

Early-Stage Design of Concrete Girder Bridges Using Set-Based Design
Parametric Exploration of Design Alternatives Considering CO_2 Emissions, Cost, and Buildability

Master's Thesis in the Master's Programme Structural Engineering and Building Technology

ALICE BEISCHER
KARIN FURUHJELM

Supervisor: Alexander Kjellgren, Skanska
Examiner: Rasmus Rempling, Department of Structural Engineering

Examensarbete ACEX30
Institutionen för Arkitektur och Samhällsbyggnadsteknik
Chalmers Tekniska Högskola, 2025

Department of Architecture and Civil Engineering
Division of Structural Engineering
Chalmers University of Technology
SE-412 96 Gothenburg
Sweden
Telephone +46 31 772 1000

Cover:
A normalized probability density distribution representing the buildability cost criterion for design solutions brought forward with the developed set-based design algorithm, together with a sketch of a two girder reinforced concrete bridge.

Department of Architecture and Civil Engineering
Gothenburg, Sweden, 2025

Early-Stage Design of Concrete Girder Bridges Using Set-Based Design
Parametric Exploration of Design Alternatives Considering CO_2 Emissions, Cost, and Buildability

Master's thesis in the Master's Programme Structural Engineering and Building Technology

ALICE BEISCHER

KARIN FURUHJELM

Department of Architecture and Civil Engineering
Division of Structural Engineering
Chalmers University of Technology

ABSTRACT

This thesis investigates the application of parametric multi-criteria optimization in the early-stage design of reinforced concrete girder bridges using a set-based design (SBD) approach. As the construction industry faces increasing pressure to reduce greenhouse gas emissions in line with Sweden's 2045 net-zero targets, methods that allow sustainable solutions in the initial stages of a project are encouraged. However, minimizing the use of carbon-intensive materials, such as concrete, can present challenges for buildability, particularly when more geometrically complex structures are introduced. To address this situation, the study incorporates both environmental impact and buildability into the optimization criteria, enabling identification of solutions that balance these potentially conflicting objectives. A developed parametric Python algorithm was used to generate a wide design space based on geometry parameters from a reference project. The study focused on cross-sections with two main girders—either of rectangular or I-shaped profiles. Each alternative was structurally verified by the algorithm through finite element analysis using BRIGADE/Plus, and subsequently evaluated in terms of investment cost, CO_2 emissions, and buildability. The analysis of over 100,000 cross-section alternatives revealed groups of material-efficient solutions that reduced both emissions and cost, although some with buildability that was negatively impacted due to increased production complexity. The results underscore the trade-offs between key criteria and demonstrate the ability of the SBD method to identify solutions that meet multiple performance targets. Overall, the study highlights the value of SBD in supporting early-stage decision-making, enabling more informed trade-offs, and reducing risk in tendering processes aimed at sustainable infrastructure development.

Key words: set-based design, parametric modeling, multi-criteria optimization, girder bridge, reinforced concrete, buildability, environmental impact

Set-baserad design i tidiga skeden av betongbalkbroars utformning
Parametrisk utforskning av designalternativ med hänsyn till CO_2-utsläpp, kostnad och byggbarhet

ALICE BEISCHER
KARIN FURUHJELM

Institutionen för arkitektur och samhällsbyggnadsteknik
Avdelningen för Konstruktionsteknik
Chalmers tekniska högskola

SAMMANFATTNING

Det här examensarbetet undersöker tillämpningen av parametrisk flerkriterieoptimering i tidiga skeden av projektering av balkbroar i armerad betong, med hjälp av set-baserad design (SBD). Byggbranschen står inför ett ökande tryck att minska växthusgasutsläppen i enlighet med Sveriges mål om nettonollupsläpp till 2045, vilket skapar ett behov av metoder som möjliggör hållbara lösningar redan i projektets inledande faser, där potentialen för effektiva implementeringar är stor. Att minimera användningen av koldioxidintensiva material, såsom betong, kan dock innebära utmaningar för byggbarheten, särskilt när mer geometriskt komplexa strukturer införs. För att hantera detta inkluderar studien både klimatpåverkan och byggbarhet som optimeringskriterier, vilket möjliggör identifiering av lösningar som balanserar dessa potentiellt motstridiga mål. En parametrisk algoritm, utvecklad i Python, användes för att generera en bred lösningsrymd baserat på geometriparametrar från ett referensprojekt. Studien fokuserade på tvärsnitt med två huvudbalkar där både rektangulära och I-balksprofiler undersöktes. Varje broalternativ verifierades strukturellt av algoritmen genom finita elementanalys i programmet BRIGADE/Plus, och utvärderades därefter med avseende på investeringskostnad, CO_2-utsläpp och byggbarhet. Analysen av över 100 000 tvärsnittsalternativ visade grupper av materialeffektiva lösningar som minskade både utsläpp och kostnader, även om byggbarheten i vissa fall påverkades negativt till följd av ökad produktionskomplexitet. Resultaten tydliggör avvägningarna mellan olika kriterier och demonstrerar SBD-metodens förmåga att identifiera lösningar som presterar väl i flera kategorier. Sammanfattningsvis tyder arbetet på att set-baserad design kan stödja beslutsfattande i tidiga skeden genom att tydliggöra kompromisser, ge bättre beslutsunderlag och minska osäkerhet i upphandlingsskedet vid utveckling av hållbar infrastruktur.

Nyckelord: set-baserad design, parametrisk modellering, flerkriterieoptimering, balkbro, armerad betong, byggbarhet, materialanvändning, CO_2-utsläpp

Contents

ABSTRACT I

SAMMANFATTNING II

CONTENTS IV

PREFACE VI

NOMENCLATURE IX

1 INTRODUCTION 1
- 1.1 Background 1
- 1.2 Aim and objectives 2
- 1.3 Limitations 3
- 1.4 Methodology 3

2 THEORETICAL FRAMEWORK 4
- 2.1 Planning and design process of infrastructure projects 4
  - 2.1.1 Importance of early-stage design optimization 5
- 2.2 Concrete bridge types 6
  - 2.2.1 Slab bridges 6
  - 2.2.2 Slab frame bridges 6
  - 2.2.3 Girder bridges 7
  - 2.2.4 Box girder bridges 8
- 2.3 Climate impact of reinforced concrete structures 8
  - 2.3.1 Carbon dioxide emission of reinforced concrete 9
  - 2.3.2 The potential to reduce material consumption 10
- 2.4 Design methods 11
  - 2.4.1 Point-based design 11
  - 2.4.2 Set-based design 12
  - 2.4.3 Parametric modeling 13
- 2.5 Multi-objective optimization 13
  - 2.5.1 Optimization criteria for environmental impact 14
  - 2.5.2 Optimization criteria for buildability 15
- 2.6 Traffic load models 18
  - 2.6.1 Traffic load models in Eurocode 18
  - 2.6.2 National vehicle model 19

3 REFERENCE PROJECT 20
- 3.1 Östrand road bridge 20
- 3.2 Modeling the reference bridge 21
- 3.3 Modifications 22

4 APPLYING THE SET-BASED DESIGN ALGORITHM 23
- 4.1 Generation of design set 24
  - 4.1.1 Rebar layout generation 25

4.2 Resistance verification 27
4.2.1 Load categories 28
4.2.2 Load combinations 29
4.2.3 Structural verification in ULS and SLS 29
4.3 Multi-criteria evaluation 30

5 RESULTS 33
5.1 Mapping of design spaces 33
5.2 Relationship between criteria 36
5.3 Comparison of sets within Design Space C 40
5.3.1 Evaluation based on girder shape 40
5.3.2 Evaluation based on concrete class 42
5.3.3 Evaluation based on rebar diamater 43
5.4 Exploration of Design Space D 43

6 DISCUSSION 47
6.1 Method discussion 47
6.1.1 Implications of excluding pre-stressing in the FE model 48
6.1.2 Buildability considerations for I-shaped girders 48
6.1.3 Assumptions and limitations in cost and buildability factors 49
6.2 Discussion of results 50
6.3 Possible further studies 51

7 CONCLUSION 53

A SOFTWARE I
A.1 BRIGADE/Plus and Abaqus I

B VERIFICATION OF FE MODEL II
B.1 Self-weight II
B.2 Traffic load III

C LOADS IV
C.1 Permanent loads IV
C.2 Variable loads IV

D VERIFICATION OF RESISTANCE VI
D.1 Serviceability limit state VI
D.2 Ultimate limit state VI
D.2.1 Bending moment resistance VI
D.2.2 Shear resistance VIII

E CRITERIA CALCULATION IX
E.1 Environmental impact cost IX
E.2 Investment cost X
E.3 Buildability cost XI

Preface

This study was conducted at the Department of Architecture and Civil Engineering at Chalmers University of Technology during the spring of 2025, as our master's thesis at the end of the Civil Engineer and the Architecture and Engineering programs. The project was carried out with the support of the Department of Bridge and Infrastructure at Skanska in Gothenburg, Sweden.

We would especially like to thank our supervisor at Skanska, Alexander Kjellgren, for supporting us throughout this process while still allowing us to take full ownership of the project. We are also grateful to the entire Department of Bridge and Infrastructure at Skanska for welcoming us and for taking the time to discuss challenges and ideas.

We are also equally grateful to our supervisor and examiner at Chalmers, Rasmus Rempling, for his experience and guidance. Our opponents, Erik and Alex, also deserve the thanks for providing valuable feedback and offering a fresh perspective throughout the entire process. Special thanks to Pontus Nyberg for generously sharing his knowledge of BRIGADE/Plus and for helping us resolve countless error messages.

Finally, we are very grateful to our families, friends, and partners for their support throughout our entire studies at Chalmers.

Gothenburg, June 2025

Alice Beischer
Karin Furuhjelm

Nomenclature

This nomenclature list presents the acronyms, design parameters, constraints, and the definitions of the design spaces used in this report.

Acronyms

CO_2	Carbon Dioxide
FE	Finite Element
FEM	Finite Element Method
FLS	Fatigue Limit State
LCA	Life Cycle Assessment
LM	Load Model
PBD	Point-Based Design
SBD	Set-Based Design
SLS	Serviceability Limit State
ULS	Ultimate Limit state

Design parameters & constraints

W	Width of bridge deck
L	Span length of bridge
MB_h	Height of main beam
MB_b	Width of main beam
Web_t	Web thickness of I-profile
Fl_t	Thickness of bottom flange of I-profile
EB_h	Height of edge beam
EB_b	Width of edge beam
ϕ, ϕ_{rebar}	Diameter of tensile reinforcement
f_{ck}	Characteristic compression strength of concrete
n_{layers}	Number of layers of tensile reinforcement
n_{bars}	Number of bars in one layer
A_s	Required reinforcement amount
δ_{max}	Maximum vertical deflection in the span

Design Spaces

Design Space A	Set of design solutions, regardless of input parameters or feasibility
Design Space B	Set of design solutions for specified input parameters, regardless of feasibility
Design Space C	Set of feasible design solutions for specified input parameters
Design Space D	Set of the 10% best performing design solutions in each optimization criteria

1

Introduction

This chapter introduces the background, aim and objectives of the thesis project, as well as covers its limitations and methodology.

1.1 Background

The construction industry is a significant contributor to global CO_2 emissions, and reducing these emissions is a crucial goal to meet climate targets. The construction sector was responsible for 22% of Sweden's greenhouse gas emissions in 2021, where new construction represents roughly 20% of those emissions (Fossilfritt Sverige, 2024). The roadmap for fossil-free competitiveness in the construction sector outlines strategies aimed at reducing the industry's carbon footprint and promoting sustainability practices, with the ultimate goal of reaching net zero greenhouse gas emissions by 2045. Thus, a key aspect of this strategy is the early integration of life-cycle consideration in the design, where consultants are encouraged to propose effective, sustainable solutions in the initial stages of a project.

There are considerable possibilities to affect a project's total climate impact in the planning and design stages. This can be achieved by implementing materials with a low carbon footprint or designs with optimized material and energy demand (Fossilfritt Sverige, 2024). For civil projects, most of the impact of the construction phase on the climate comes from materials, where asphalt, concrete, and steel contribute up to 80%. Thus, a design of optimized material use contributes to strategies to reach net zero greenhouse gas emissions.

Buildability is also a critical factor in the construction sector. It is defined by the Construction Industry Research and Information Association (CIRIA) in the UK as "the extent to which the design of a building facilitates ease of construction, subject to the overall requirements for the completed building" (Wimalaratne et al., 2021). Buildability involves integrating construction knowledge and experience throughout the project delivery process to achieve overall project objectives, such as cost, quality, productivity, safety, and timely completion. It can also be defined as a process that promotes design that facilitates building construction. Although it is recommended to incorporate the aspect of buildability throughout all phases of a construction project, the design phase is considered critical to implement buildability. Thus, structural designers have a significant responsibility to include buildability in the project.

In practice, aiming for environmental sustainability in a construction project must be balanced with buildability. When these two objectives are successfully incorporated, design solutions with a reduced climate impact and a high level of buildability could possibly be found. One promising approach to achieving this balance is set-based de-

sign (SBD). SBD is an approach that maintains a wide range of design options as long as possible during the design process (Nahm and Ishikawa, 2005). Instead of narrowing down to a single solution early in the process, SBD allows simultaneous exploration of multiple alternatives and criteria, such as buildability and material reduction. This approach is particularly beneficial in structural engineering, where it allows the consideration of various design criteria and input from stakeholders before finalizing the optimal solution (Rempling et al., 2019). Finding solutions that have a high degree of buildability and sustainability is a priority for contractors who often work with design-build contracts.

Recent research has explored the application of set-based design in bridge engineering to balance sustainability and buildability. For instance, Bergenram and Ulander (2023) implemented a parametric multi-criteria optimization approach for slab frame bridges, considering investment cost, environmental impact, and buildability. Their findings indicated that while environmental impact could be reduced by up to 13.7%, this often came with a slight increase in costs due to buildability considerations. Similarly, Mathern et al. (2018) proposed a conceptual framework integrating sustainability, buildability, and performance in structural design, emphasizing the importance of informed decision-making in early design stages. These studies highlight the potential of SBD in optimizing bridge designs but also reveal limitations. Notably, much of the existing research focuses on slab frame bridges, leaving a gap in the application of SBD to other bridge types, such as concrete girder bridges. Furthermore, while buildability is acknowledged as a critical factor, there is a lack of comprehensive methods to quantitatively assess it within automated design processes. This study aims to address these gaps by exploring the implementation of SBD with parametric calculation models in the early design of concrete girder bridges, evaluating design solutions based on both buildability and CO_2 equivalents.

1.2 Aim and objectives

The purpose of the study was to explore the possibility of implementing set-based design with parametric calculation models in the early design of concrete girder bridges, evaluating the generated design solutions based on buildability and CO_2 equivalents. Thus, the objectives of the project were to:

- Explore the potential of digital and automated design workflow in early-stage bridge design,
- Implement multi-objective optimization on the cross-section of a reinforced concrete girder bridge, to explore trade-offs between climate impact, buildability, and investment cost,
- Investigate how buildability aspects can be incorporated into the automated design process for girder bridges, and to
- Assess whether the proposed method can generate design solutions with reduced climate impact.

1.3 Limitations

The study was limited to reinforced concrete girder bridges. The environmental impact considered was limited to the impact of the material since the differentiating factors between the different designs were the cross-sectional area and thus the amount of material. Quantitative measurements of buildability were investigated and based on previous studies.

To evaluate the climate impact of bridge designs, the impact has been limited to only the amount of concrete and reinforcement steel in the bridges. This included only the superstructure, excluding abutments and details such as guardrails. Several bridge life cycle assessment (LCA) studies show that the dominant materials in climate impact are concrete, reinforcement steel, and construction steel (Uppenberg et al., 2017). In addition, asphalt can also have notable climate impact in the total life-cycle (Hammervold et al., 2013). However, the amount of asphalt used for each bridge design is assumed to not differ significantly, making it a less interesting aspect to include. In conclusion, the environmental impact calculations in the study were limited to the impact of the reinforced concrete material of the superstructure.

Also, any required foundation work was excluded from this study. It is a variable that varies for every situation, making it a complex problem with the work load becoming a study of its own (Uppenberg et al., 2017). Thus, although foundation work, like piling, are common and can also contribute to a significant part of the total environmental impact in bridge construction, it was excluded from the study.

Since the method was intended to facilitate in the early design process, full dimension checks were not included in the structural verification. Some limitations were made to reduce the computational work. The designs were verified for bending moment and shear in ULS and deflection in SLS to be considered feasible solutions.

1.4 Methodology

In the initial stage of the project, a literature study was carried out exploring relevant fields of research and obtaining knowledge on nearby topics, such as parametric design and bridge types.

The main part of the project work was to develop a set-based multi-criteria optimization algorithm for bridge design, focusing on generating, verifying and evaluating design alternatives. The process involved finite element modeling (FEM) for structural verification, and the optimization criteria were centered on environmental impact and buildability. A reference project was chosen to guide the process. Digital tools were integral to the methodology, with Python employed for algorithm development and data handling. The finite element analysis was conducted using BRIGADE/Plus, enabling precise structural assessments of the generated design alternatives. The approach prioritized the systematic generation of extensive design datasets, which allowed for the exploration of complex cross-sectional geometries and efficient handling of large data sets. This, in turn, provided supported for informed decision-making in the design process.

2

Theoretical Framework

In this chapter, theoretical background is provided on topics covered in the thesis. Initially, information about the the design processes related to infrastructure projects is included. Followed by information on bridge types and the climate impact of constructing civil projects. Further, the load categories that apply are described, as well as an exploration of different design methods. Lastly, the multi-objective optimization and its criteria are explained.

2.1 Planning and design process of infrastructure projects

The Swedish Transport Administration has determined a project process for large infrastructure projects, where both climate calculations and economic calculations are required in multiple steps of the process (Miliutenko, 2022). The planning and design process of infrastructure projects, such as bridges, is comprehensive and involves multiple stages and stakeholders, see Figure 2.1.

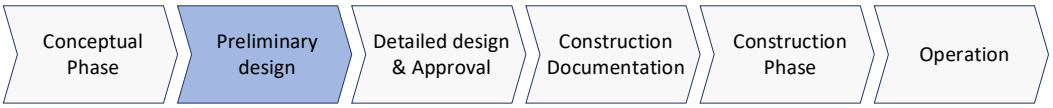

Figure 2.1: The Swedish Transport Administration's process for developing infrastructure, with the studied phase highlighted.

The process can be divided into the following phases:

Conceptual design: The process begins with identifying the need for the infrastructure project by considering factors such as traffic demand, urban development, safety, and environmental impact (Eriksson, 2013). A feasibility study is conducted to assess the technical, economic, and environmental viability of the project, including initial climate calculations using the tool *Klimatkalkyl* for projects with a total cost of $\geq$ 50 million SEK (Miliutenko, 2022). Often in this initial phase, different alternatives with respect to location, routing, and design are explored and presented on a conceptual level. Roughly estimated calculations are used to analyze how different choices affect the project's climate performance and economic cost. The stakeholders involved provide input for evaluating the risks and concerns with the specific project going forward.

Preliminary Design: In this phase, the project design is further refined. More detailed design plans that include technical specifications are part of the consultation materials produced in this stage, along with Environmental Impact Assessments (EIA). EIA are

developed to determine the significant environmental impact of the project (Trafikverket, 2022). Conducting more detailed financial evaluations to assess the project's economic feasibility is also part of this phase, in a cost-benefit analysis.

Detailed design and Approval: The final engineering designs feature comprehensive and detailed design plans, including all technical specifications and construction details (Trafikverket, 2022). Another climate calculation is included in the decision-making materials for approval. Obtaining all necessary permits and approvals to proceed with construction is also part of this phase.

Construction Documentation: This phase involves preparing detailed plans for the construction process, including timelines and resource allocation, as well as other documents for the procurement of contractors and suppliers (Eriksson, 2013). The climate calculation is aligned with the latest economic data which serves as the basis for the tendering process.

Construction and Operation: In the final phases, along with constructing and operating the project itself, compiling a climate declaration is part of the project's final report (Miliutenko, 2022). This declaration includes the actual climate impact of the project and is used to monitor and improve climate efficiency in future projects.

This approach ensures transparency in the planning and design of infrastructure while considering environmental impacts. The use of the Klimatkalkyl tool throughout the process helps maintain consistency and allows for ongoing refinement of the climate calculations as the project progresses.

The iteration in performing climate calculations can be aided by using an automated design flow, such as set-based design (Hansson & Tacking, 2024). With the design and calculated climate impact automatically adjusting when a parameter is changed, significant time can be saved. The uncertainty involved in decision making in the preliminary phase is also managed through the use of set-based design.

2.1.1 Importance of early-stage design optimization

In early project phases, the potential for optimization is greater while the cost of making changes are lower (Bragança et al., 2014). The possibility of influencing cost and environmental impact is high in the early design phase, while the cumulated impacts and costs are still low, see Figure 2.2. This relationship changes throughout the construction's life time, and late changes will cost more both economically and environmentally. Thus, optimization of a design is most effective in the early stages of a project and is substantial in creating solutions with low environmental impact and achieving climate goals.

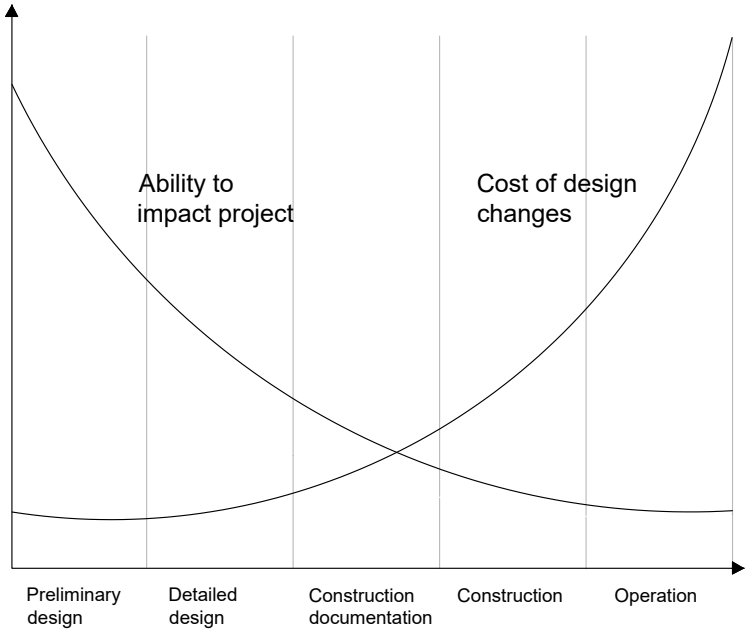

Figure 2.2: How the ability to change the design correlates with the cost according to the Macleamy curve.

2.2 Concrete bridge types

Different types of bridges offer specific advantages, making them more suitable for certain applications (Kettil, 2023). This section provides an overview of the most commonly constructed concrete bridges in Sweden with short to medium spans, including the cross-section types evaluated in this study.

2.2.1 Slab bridges

Slab bridges consist of a solid reinforced concrete slab that spans between supports (Concrete Bridge Development Group, n.d.). The construction of slab bridges is typically straightforward and cost-effective. The slab distributes loads uniformly in all directions, making it suitable for small to medium-sized bridges.

Figure 2.3: A slab bridge's typical shape of the bridge deck.

2.2.2 Slab frame bridges

Slab frame bridges are an extension of slab bridges, incorporating a frame structure to provide additional support and stability (Yavari, 2017). These bridges are often used in

urban areas where space is limited and complex load conditions are present. The frame structure, including frame legs and wing walls, allows for better distribution of loads. This bridge type is very common in Sweden and has been a subject for set-based design in previous studies (Bergenram & Ulander, 2023)

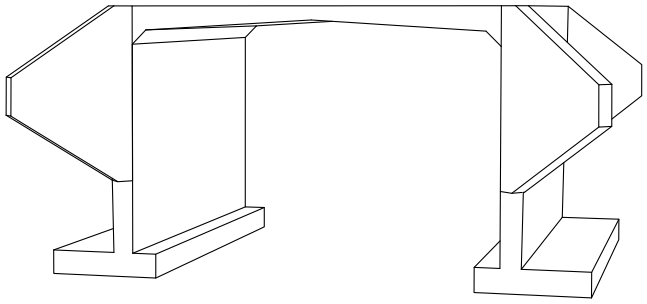

Figure 2.4: Typical appearance of a slab frame bridge.

2.2.3 Girder bridges

Girder bridges are among the simplest and most common bridge types, using beams, also called girders, to support the bridge deck (Concrete Bridge Development Group, n.d.). These girders can be made from either steel or concrete with various cross-section shapes, such as I-girders or rectangular cross-sections. The straightforward design of girder bridges allows for rapid construction and cost-effectiveness, especially for short to medium spans. Concrete girder bridges with span lengths over 30 meters are typically pre-stressed (Kettil, 2023).

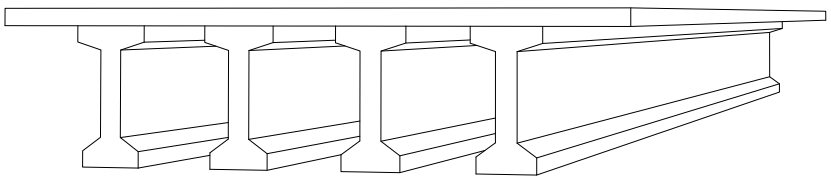

Figure 2.5: Girder bridge with I-shaped girders.

I-shaped girders are considered more material-efficient than rectangular cross-sections, as they require approximately 20% less concrete per square meter of bridge deck to achieve the same structural capacity (Kettil, 2023). This efficiency makes them a favorable option in terms of material consumption and environmental impact. However, their more complex geometry introduces challenges in the form of intricate reinforcement detailing and more demanding formwork. As a result, I-girders are most commonly

used in prefabricated beams, where minimizing the weight of structural elements is essential for transportation and lifting. In some cases, these prefabricated I-beams may also be applied in girder bridges, depending on project-specific constraints and logistic considerations.

The production techniques used in prefabricated I-girders can also be adapted for in-situ construction, particularly in medium-span bridges (Kettil, 2023). In such cases, reinforcement must be completed before the formwork is assembled around the girder, and the top surface of the bottom flange should be sufficiently inclined to prevent air pockets from forming during casting. Although feasible, this process adds complexity to construction and generally requires more labor time compared to bridges using rectangular girders. If the girder geometry can be standardized to allow for reusable formwork across multiple spans or projects, it may help reduce formwork costs and material use. Ultimately, while I-girder bridges can offer material and environmental benefits, these advantages must be carefully weighed against increased construction complexity, labor effort, and associated costs.

2.2.4 Box girder bridges

Box girder bridges are characterized by their hollow box-shaped cross-sections, typically constructed from prestressed concrete (Concrete Bridge Development Group, n.d.). The void ensures that the material is used where it is most effective. Multiple shape variations exist for the box cross-section, such as trapezoidal or square boxes. It is also possible for the box girder depth to vary along the span. This advanced cross-sectional design provides high torsional stiffness and strength, making box girder bridges particularly suitable for spans longer than 45 meters, curved alignments, and complex load conditions. The enclosed structure also offers better protection against environmental factors, reducing maintenance needs. However, the complexity of their design and construction can lead to higher costs compared to simpler bridge types.

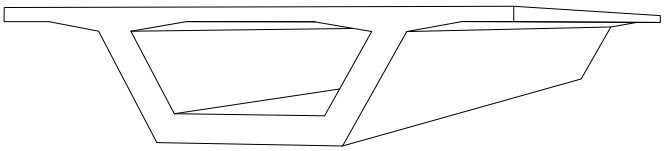

Figure 2.6: Box bridge with a trapezoidal box shape.

2.3 Climate impact of reinforced concrete structures

Reinforced concrete has many applications and is the most widely used construction material in the world (Lea & Mason, 2025). However, the production of concrete and steel used in bridges accounts for a substantial share of total emissions from infrastructure construction (Uppenberg et al., 2017). These emissions are commonly referred to as *embodied carbon*, which encompasses the total greenhouse gas emissions arising from the extraction, processing, transportation, and manufacturing of construction materials. Understanding the sources and magnitudes of these emissions is beneficial in

evaluating the climate impact of concrete structures and identifying opportunities for improvement. This section provides an overview of the carbon dioxide emissions associated with reinforced concrete, followed by an exploration of strategies to reduce its environmental footprint through material efficiency and design optimization.

2.3.1 Carbon dioxide emission of reinforced concrete

Cement is a key ingredient in concrete, but is also an enormous contributor to its CO_2 emission (Lea & Mason, 2025). Figure 2.7 shows an example of how the components of a typical concrete mix contribute to its carbon footprint. The manufacture of cement is a significant contributor to global warming, as 4–8% of the world's carbon dioxide emissions are estimated to come from its production. The step in the production process of burning raw materials in a kiln to produce cement clinker, and the carbon dioxide directly emitted from this chemical reaction, called calcination, is more than half of the total emission of cement production. Possible actions to reduce the emissions of cement production could be the introduction of renewable energy to replace fossil fuels in the manufacturing process, increasing the energy efficiency of cement plants, carbon capture and storage, and reducing the amount of portland cement needed by adding supplementary cementious material (SCM) such as blast furnace slag or fly ash. From another perspective, reducing the material consumption of concrete itself by increasing structural efficiency could also be a possible action to reduce the CO_2 emissions of concrete in the building industry.

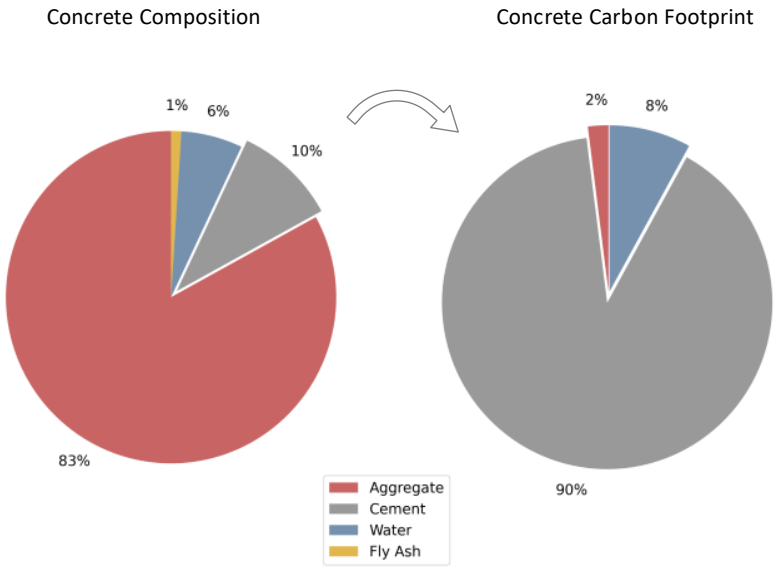

Figure 2.7: Components of a concrete mix and their corresponding share of the material's carbon footprint. Redrawn from (Niveditha et al., 2020).

In addition to cement, reinforcing steel is a significant contributor to the climate impact of reinforced concrete structures due to its high embodied carbon. Among construction materials, reinforcing steel emits the most CO_2 per unit weight (Kwon et al., 2021), about 9.2 times that of concrete class C25/30, for example. On a global scale, the steel

sector is responsible for an estimated 6–7% of total greenhouse gas emissions (Sheng et al., 2024). A major source of these emissions is the energy-intensive blast furnace-basic oxygen furnace (BF-BOF) production route used in manufacturing virgin steel. The process involves iron ore and coal at high temperatures and generally burns natural gas as energy that also emits significant amounts of CO_2. Although reinforcement bars are typically made of 90-100% recycled steel, the recycling process of steel still has a significant environmental burden, although it is lower than virgin steel (Purnell, 2013). This underlines the importance of including reinforcing steel in environmental assessments of concrete structures, especially when moving from material-level data to evaluating the total embodied carbon of entire structural systems

Estimating the embodied carbon of reinforced concrete is complex (Purnell, 2013). Cement and reinforcing steel have the biggest contributions out of the components in reinforced concrete, while aggregate, water, and admixtures have minimal influence. Depending on the design requirements and the structural component studied, the proportions of these five components can be altered to obtain different structural properties. A study by Purnell (2012) has shown that structural design and loading are the main influences on the embodied carbon of reinforced concrete (Purnell, 2013). For comparison, the embodied carbon of plain concrete is instead strongly dependent on the mix design and its compressive strength. Thus, both concrete and reinforcing steel are parameters where optimization enables the possibility to reduce the total CO_2 emissions of reinforced concrete structures.

2.3.2 The potential to reduce material consumption

In a study funded by SBUF (Development Fund of the Swedish Construction Industry), the goal was to establish construction solutions with "optimized" geometries that result in significant material savings and thus reductions of CO_2 emission, compared to the standard cross-section designs. These solutions were also required to meet the functional requirements and be compatible with production methods that ensure reasonable time frames and costs. The report, "Climate-optimized Concrete Bridges – Geometry and Material" (Kettil, 2023), shows that concrete volumes, can be significantly reduced, by approximately 30%, while still meeting functional requirements. In some cases, deviations from the bridge standard may be necessary, but this can still be accepted by demonstrating that the alternative solution meets the required function. In addition, combining the material-efficient geometries of the study with so-called "green concrete", concrete containing SCM and less cement, could lead to CO_2 reductions up to 50%. A proposed reason for why this approach is not currently implemented is that the increased production cost is considered to outweigh the material savings. This point again highlights the need to find solutions with low climate impact without compromising on buildability factors.

A recent study by Björnsson et al. (2025) found that the material consumption of concrete bridges in Sweden has increased in the last 50 years and investigated the reason for this increase. Although investigations indicate that different factors contribute, a general conclusion was that the development of design codes and engineering practices has had a significant impact on increased material consumption. For example, traffic loads have increased, while durability requirements have become stricter. Also, how engineers analyze structures has developed over time, with increased use of 3D FEM over analytical calculations. The study also aimed to investigate whether these devel-

opments are justified. However, drawing a definitive conclusion on whether an increase in material consumption leads to better performance or is a waste of material proved to be difficult.

Some mitigating measures suggested by Björnsson et al. (2025) to reduce the trend of increasing material consumption are to challenge and clarify code provisions and to encourage both conceptual thinking among engineers and the courage to question design codes when justified. Björnsson et al. (2025) further specifies that, although the transition to greener material alternatives reduces the environmental impact of a structure, it is not enough to focus solely on that. To further reduce the environmental footprint, it is necessary to focus on how to systematically reduce material consumption. In addition, Björnsson et al. (2025) mention that the choices made in the early design process have a big impact on the material consumption of the structure, meaning that early choices could, for example, "lock in" geometries and other structural boundary conditions which limits the possibility of saving on material in later design stages. This problem could SBD help with, through its possibility of exploring multiple design alternatives in the early design process before finalizing the chosen solution, enabling comparison between design alternatives of different material consumptions.

2.4 Design methods

This section introduces the traditional and most commonly used design method in the field of structural engineering today, point-based design, as well as the more recently developed methods of set-based design and parametric design, which are both used in combination in the thesis work.

2.4.1 Point-based design

The traditional design method used in structural engineering is often called point-based design (PBD), as it is based on a single design option selected early in the process (Parrish et al., 2007). The chosen design is then refined in more detail as new information arises throughout the project, see Figure 2.8. Taking into account the multiple stakeholders that place demands on the outcome, this method requires an iterative rework of the chosen design (Parrish et al., 2007; Mathern et al., 2018). The decision-making process in structural engineering, and thus in point-based design, is typically driven by the judgment, based on experience, of the engineers involved (Fernández and Ramos, 2014). However, the perspectives of other stakeholders are generally not considered, which can result in solutions that, while technically feasible, are suboptimal in other terms, such as cost, environmental impact, or buildability. The additional work due to the need for rework as well as the inability to cater to multiple criteria simultaneously are reasons why the point-based design method is deemed ineffective.

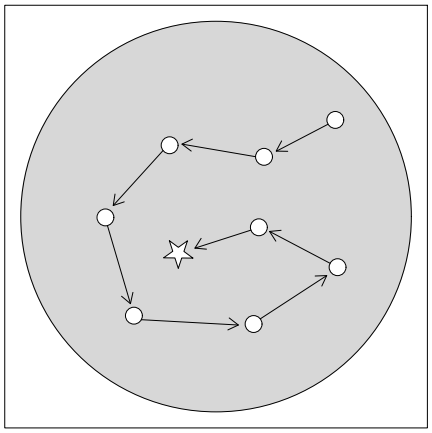

Figure 2.8: Schematic figure of the point-based design process. Arrows represent design decisions made and small circles the new design. The star represents the final design.

2.4.2 Set-based design

Improving the buildability and performance of structures while simultaneously reducing their economic and environmental impact has become a topic of greater interest in recent years (Mathern et al., 2021). Set-based design (SBD) allows the exploration of many design solutions and the evaluation of them against the objectives of the project, thus giving the possibility to find the most appropriate designs.

Set-based design considers a set of design options from the beginning, instead of preferring a single solution as in PBD (Parrish et al., 2007). This approach allows maintaining a broad *design space* as long as possible and allows decisions to be postponed, thus minimizing the need for rework. A valued benefit and incentive for the development of the method is the economic precaution to avoid a complete redesign late in the process. In comparison, there is a risk with point-based design, where significant new learning points that arise later in the timeline require a complete redesign to meet updated demands. However, in SBD, the design space is narrowed down as new criteria are introduced during the process. There is also the possibility to revisit previous choices since all design options within the sets remain available, allowing for an ongoing comparison of alternatives. A crucial aspect of SBD is that the criteria that eliminate options from the design set are well defined and documented (Parrish et al., 2007). The idea behind this is to keep all stakeholders informed about decisions made and to easily reacquire design sets that are disregarded in case of elimination criteria shifting.

A study by Bergenram et al. (2024), on multi-criteria optimization of slab frame bridges, structured the SBD algorithm into four design spaces, labeled A through D. A similar approach to design spaces was used in this study, as illustrated in Figure 2.9. Design Space A was the initial and largest design space, covering all possible bridge cross-section designs, regardless of feasibility. Design Space B refers to the set of designs within Design Space A that defined by the established governing geometry input parameters for the structure. Of this set, a check of technical feasibility is made through ULS and SLS verification. Thus, Design Space C only includes the designs that meet these constraints. What separates Design Space D from the previous is the filtering

through multiple criteria such as cost, environmental impact, and buildability. The final Design Space D consists of the designs optimized according to selected criteria. This structure is one of several possible approaches to implementing SBD, and the specific formulation of design spaces can be adapted to suit the objectives and context of a given study.

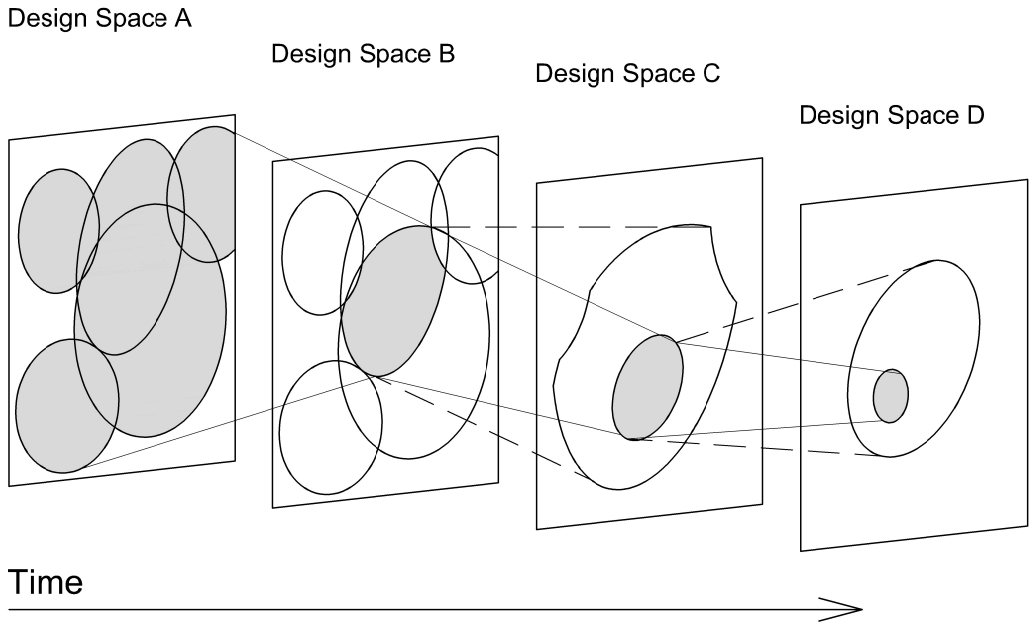

Figure 2.9: A visual representation of the set-based design method.

2.4.3 Parametric modeling

Parametric modeling is a common design practice within computer-aided design (CAD), which is used in a variety of design fields such as architecture, structural engineering and product design. The demand for flexible design tools within these fields is what drove the inclusion of parametric modeling in various design software (Hernandez, 2006).

Parametric modeling easily allows for variations when working on a design, without the need to erase or rework. This flexibility is possible due to the ability for users to define adjustable parameters and rules with respect to different attributes of the design. Changing a parameter subsequently reconfigures all linked design functions performed in the software and gives the user immediate visual feedback on the change of input. One prominent area of use for parametric modeling is to generate multiple design options (Lee and Ostwald, 2020). This process can be automated and controlled through the algorithmic functions of parametric design tools, such as Grasshopper. Creating a large number of design solutions with this method can hence be utilized as a design set used in set-based design to further automatize that process.

2.5 Multi-objective optimization

Multi-objective optimization aids in maximizing the utility values of various potentially conflicting objectives (Mathern et al., 2021). It is common in engineering problems that

different objectives will, to some degree, contradict each other, resulting in no single correct solution which satisfies all objectives. Multi-objective optimization aids in the compromising between objectives.

An optimization problem can mathematically be expressed by the general formulation in equation (2.1) (Yavari et al., 2016; Khouri Chalouhi, 2019). *Objective functions* $f_i(\mathbf{x})$, *constraint functions* $g_j(\mathbf{x})$ and $h_k(\mathbf{x})$, and *design variables* $\mathbf{x}$ are used to define an optimization model to find the optimal solution.

$$\begin{aligned} \text{minimize} \quad & f_i(\mathbf{x}), && i = 1, 2, \ldots, M \\ \text{subject to} \quad & g_j(\mathbf{x}) \leq 0, && j = 1, 2, \ldots, J \\ & h_k(\mathbf{x}) = 0, && k = 1, 2, \ldots, K \\ \text{where} \quad & \mathbf{x} = [x_1, x_2, \ldots, x_n] \in \mathbb{R}^n \end{aligned} \tag{2.1}$$

The objective functions describe the objectives and intentions of the project. Relevant objectives for a building or civil engineering project are related to the economy, the performance of the structure, the environmental impact and the buildability (Mathern et al., 2021). Examples of objectives are to reduce the construction cost, minimize the deflection of structural elements, and reduce the construction time and CO_2 emission of a project. In addition to objective functions, constraints and design variables are needed to construct an optimization model. Objective functions can be understood as mathematical formulations of the *optimization criteria*, serving as tools to evaluate and compare design alternatives in relation to defined goals.

Constraint functions and design variables limit and define the design problem (Mathern et al., 2021). Structural norms and standards establish the constraints in structural design with the intention of the construction to be structurally sound. The design effects of loads are determined by appropriate structural and load models, that should be within the limit of the associated design constraint. The design variables, also called design parameters, and their possible values define the design problem and generate a design space of possible configurations. Concrete class, element dimensions, and diameter of reinforcement bars are examples of design variables in the context of this study. With the objectives, constraints, and design variables defined, an optimization model can be defined for a set-based design process.

2.5.1 Optimization criteria for environmental impact

The objective function for an optimization criterion of the environmental impact can be described by the environmental impact of each relevant material (Yavari et al., 2017). As described in Sections 1.3 and 2.3.1, concrete and reinforcing steel dominate the total CO_2 emissions of reinforced concrete bridges and where the possibility of optimization is the highest. The environmental impact of a bridge can then be simplified to include only the effect of these two materials in the preliminary design phase.

In a study by Yavari et al. (2017), the environmental cost of reinforced concrete was assessed using a detailed life cycle assessment with the ReCiPe midpoint method and two monetary weighting systems to convert environmental impact to monetary cost. The ReCiPe midpoint method is the most comprehensive LCA methodology currently available and includes 11 types of impact categories. The study by Yavari et al. (2017) chose to include six of these impact categories due to the "limited availability of mon-

etary values in practice", and only impact categories with indicators available in both investigated weighing methods. These impact categories in the LCA covered not only green house gas emissions, but also parameters related to ecosystem quality, resources and human health.

Through a cradle-to-grave LCA, the study by Yavari et al. (2017) produced characterized values of the environmental impacts of three common concrete strength classes and reinforcement, using the Ecoinvent version 3 database. The two monetary weighting systems investigated and compared by Yavari et al. (2017) were Ecovalue12 and Exotax02. The Ecovalue weighting system is derived from the reduction in benefits resulting from environmental deterioration, with a focus on Swedish conditions (Finnveden et al., 2013). The Ecotax set is "based on environmental taxed and fees" (Yavari et al., 2017). However, the results of the study show that both weighting systems yield the same optimized results in total.

Finally, the objective function for the environmental optimization criterion was defined as in equation (2.2) (Yavari et al., 2017).

$$f(x) = EnvCost_{concrete} + \alpha_{reb} \times EnvCost_{reinforcement} \tag{2.2a}$$

$$EnvCost = \sum_{i=1}^{n} impact_i \times monetary_i \tag{2.2b}$$

where $EnvCost$ is the total associated environmental cost of the n number of impact categories, $impact_i$ is the impact based on the characterized environmental impacts for the i'th impact category and $monetary_i$ is the associated environmental cost of $impact_i$ based on the Ecovalue or Ecotax monetary weighting factors. To consider additional reinforcement needed in design details and anchorage length, α_{reb} was introduced, based on practical experience in design, set equal to 1.4.

This method of defining environmental optimization criteria presented by Yavari et al. (2017) was able to be efficiently applied to the design process of slab frame bridges. This work was also supported by another study by Bergenram and Ulander (2023) who implemented the same method with confirmed results.

2.5.2 Optimization criteria for buildability

Buildability has several positive impacts on the outcome of construction projects. A high degree of buildability results in benefits not only for the outcome of the project, but also for the client and the construction organization (Osuizugbo et al., 2023). Buildability is shown to be economically, safety and quality beneficial, see Figure 2.10.

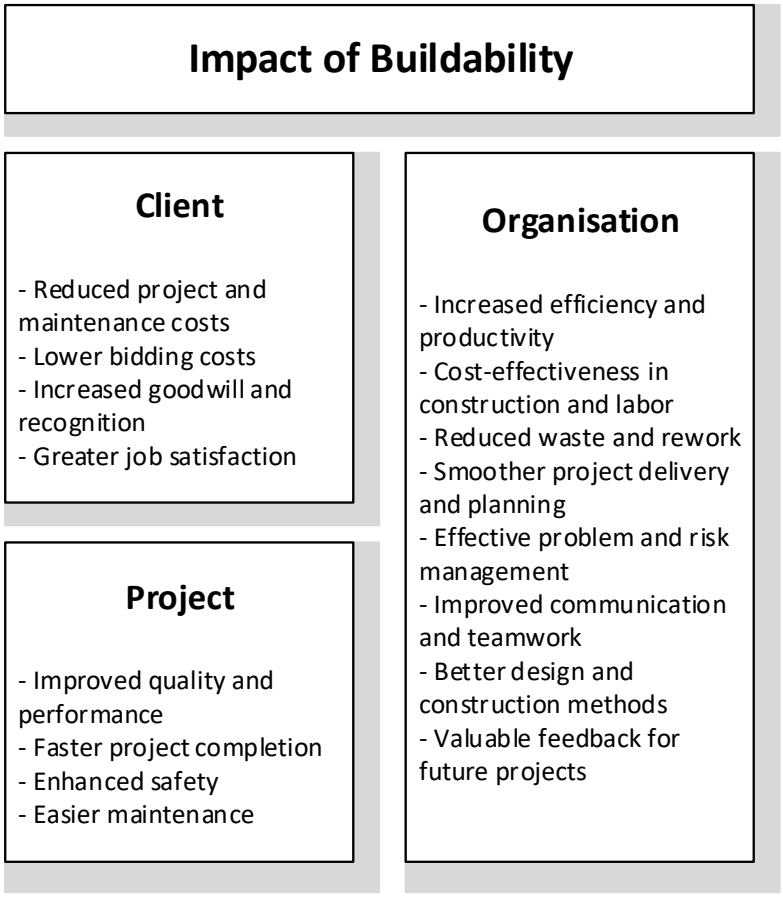

Figure 2.10: Possible impact of buildability according to (Osuizugbo et al., 2023).

The concept of buildability needs to be discretized into measurable quantities to enable its implementation into an optimization model. Buildability is a complex concept with numerous aspects concerning what is feasible and efficient during construction (Osuizugbo et al., 2023). A study by Yavari et al. (2016) investigated the possibility of optimizing the investment cost when building slab frame bridges, where the investment cost included the cost of material, the procurement cost and the production cost. When both labor and material costs are considered, there is the possibility of also quantifying and implementing aspects of buildability in an optimization model (Bergenram & Ulander, 2023). Yavari et al. (2016) defined an objective function based on the material and labor costs of concrete, formwork, and reinforcement, see equation (2.3), and presented unit prices for different construction processes.

$$f(x) = Cost_{concrete} + Cost_{formwork} + \alpha_{reb} \times Cost_{reinforcement} \tag{2.3}$$

The factor α_{reb} accounts for the additional cost associated with increased reinforcement amounts due to anchorage lengths and detailing, and was set equal to 1.4.

The study by Yavari et al. (2016) implemented three aspects of buildability into the objective function for their cost optimization:

- The thickness of the structural members was assumed to affect the buildability,

as a thinner concrete section involves larger amounts and more dense reinforcement, resulting in more labor hours and longer construction time. This was implemented by a factor that increased the labor cost of the reinforcement.

- Varying thickness of the structural members was assumed to increase both the cost of the formwork and the reinforcement work, increasing labor costs compared to members of constant thickness. This aspect was implemented by a factor that increased the cost of formwork and reinforcement labor.
- A concrete mix of a higher strength class was assumed to increase the labor time due to its less workable properties. This was implemented by adding an additional cost per volume for concrete class C50/60 and higher.

Based on the study by Yavari et al. (2016), Bergenram and Ulander (2023) further developed a definition of measurable buildability criteria, since both studies focused on the implementation of an optimization algorithm on slab frame bridges. Bergenram and Ulander (2023) interviewed a structural engineer specialist and a calculation engineer at Skanska to further study the possible interpretations of the buildability criteria. In reality, buildability is assessed by capacities related to different tasks, "ultimately adjusting the number of labor hours needed to finish certain production procedures" (Bergenram & Ulander, 2023, p. 31). The labor hours differ from different construction processes; what type of structural element is being casted, the properties of the reinforcement, the transporting conditions, the climate on site, and factors of the surroundings. However, some of these aspects do not correlate with the design of the bridge and cannot be taken into account when optimizing the design solution (Khouri Chalouhi et al., 2019). The relevant factor is the time required to build an element, which is related to the amount of material and the complexity of the element. The time to erect an element can vary significantly depending on the shape and function of it. Consequently, buildability criteria suitable for integration into optimization frameworks should be limited to quantifiable design-related parameters that influence the duration and complexity of the production.

From the recommendation of experienced professionals working at Skanska, Bergenram and Ulander (2023) implemented two additional buildability aspects in their objective function in comparison to the study by Yavari et al. (2016). In interviews, they found that the addition and anchorage of shear reinforcement increases labor costs. In addition, smaller diameters of reinforcement bars correspond to more hours of placement due to the increased number of bars needed to reach the same unit volume as larger diameters. Both of these buildability aspects were implemented, respectively, by a factor that increased the labor cost of the reinforcement. Bergenram and Ulander (2023) ultimately defined the buildability cost for a bridge design as:

$$\begin{aligned} cost_{build} = cost_{build,var} + cost_{build,sl} + cost_{build,conc,class} + \\ \alpha_{reb} \times (cost_{build,\phi} + cost_{build,stirrup}) \end{aligned} \tag{2.4}$$

In addition to the buildability aspects mentioned above, Khouri Chalouhi (2019) describes that the type of cross-section affect the buildability. Different shapes of the elements has a consequence on the labor cost for the same amount of material, because the reinforcement work difficulty increases, and thus takes longer. Figure 2.11 displays an example of three different cross-section types with increasing reinforcement labor hours for every cross-section type presented.

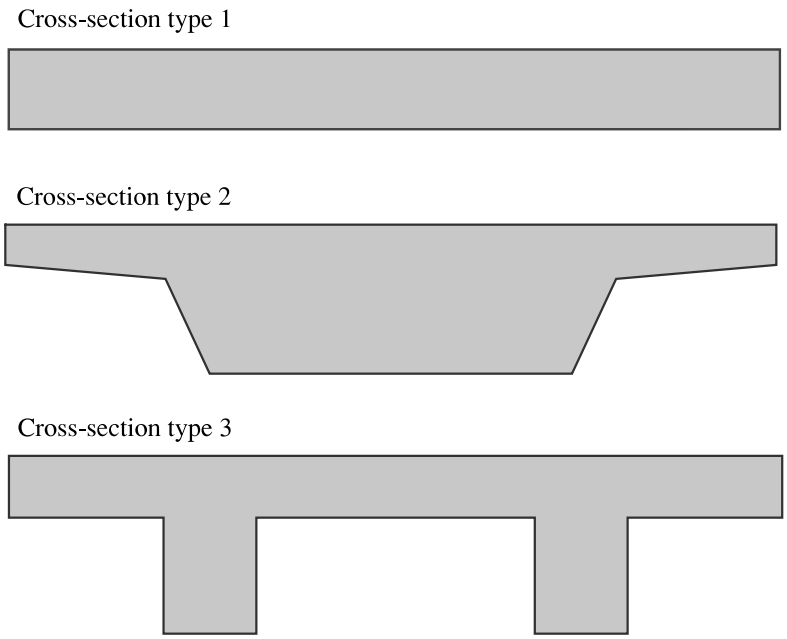

Figure 2.11: Examples of different cross-section types with varying buildability due to their shape, illustration inspired by (Khouri Chalouhi, 2019).

2.6 Traffic load models

In Sweden, the design of road bridges must comply with the European Standard, Eurocode SS-EN 1991-2 (Swedish Institute for Standards, 2011), and the regulations set forth by the Swedish Transport Agency (Transportstyrelsen, 2018). In this section, the focus is on the traffic loads that affect the superstructure. This includes four Load Models (LM) according to Eurocode and a National Vehicle model according to the Swedish Transport Agency.

2.6.1 Traffic load models in Eurocode

According to SS-EN 1991-2 (Swedish Institute for Standards, 2011), traffic loads from cars, lorries, and special vehicles produce static and dynamic forces. Simplified load models are applied to represent real load situations. Traffic actions can include vertical loading, horizontal acceleration and braking forces, and centrifugal forces from asymmetrical loading across the bridge deck.

The load models for vertical loads presented in Eurocode are as follows:

- Load Model 1 (LM1): Concentrated and uniformly distributed loads, which cover most of the effects of the traffic of lorries and cars. This model should be used for general and local verifications.
- Load Model 2 (LM2): A single axle load applied on specific tire contact areas which covers the dynamic effects of normal traffic on structural members of length 3 m to 7 m.
- Load Model 3 (LM3): A set of assemblies of axle loads representing special

vehicles (e.g. for industrial transport) which can travel on routes permitted for abnormal loads. It is intended for general and local verifications.

- Load Model 4 (LM4): A crowd loading, intended only for general verifications.

2.6.2 National vehicle model

In the national vehicle model, several load cases (A-O) are involved, as outlined by the Swedish Transport Agency (Transportstyrelsen, 2018). These cases should be tested individually, with the vehicle placed in the most unfavorable position. The vehicle can occupy a maximum of two load fields with loading factors of 1.0 and 0.8, respectively. Additional load fields, if present, are subjected to a uniform load of 0 or 5 kN/m.

3

Reference Project

A reference project was chosen from Skanska's archive and acted as a base for the generation of the design set, where the geometry of the bridge was used as a base point from which to proceed with optimization. The study was also limited to the analysis of the superstructure, excluding the supports and foundation. First, an FE model was created based on the superstructure of the reference project. Secondly, support reactions, deflection, bending moment, and shear forces were compared with the calculation report of the reference project to verify the FE model. In addition, analytical calculations also supported the verified model. Verifications are expanded on in Appendix B.

In addition, during the production of the FE model, a macro recorded the modeling. The macro script was then parameterized in preparation for the SBD algorithm. This chapter describes the reference project, how the FE model was made, and the modifications made from the reference project to the model.

3.1 Östrand road bridge

The selected reference bridge was the Östrand road bridge – a two-lane road bridge spanning four railway tracks on the Swedish east coast, close to Sundsvall. It is a simply supported girder bridge on traditional concrete abutments, see Figure 3.1. The bridge has a span of 35.5 meters and a deck width of 9.0 meters. The superstructure was constructed by in-situ casted reinforced concrete and consists of a bridge deck with edge beams and two prestressed main beams, as illustrated in Figure 3.2. The concrete used in the superstructure is of strength class C32/40. The reinforcement bars are of type B500B. In addition, three cross beams in reinforced concrete stabilize the superstructure.

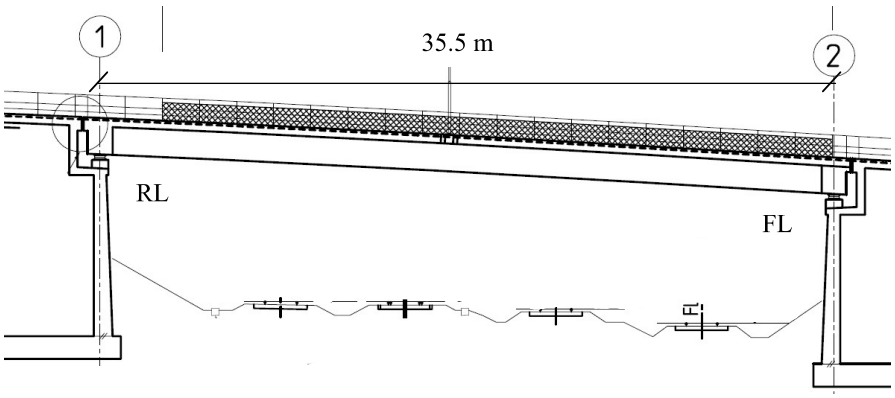

Figure 3.1: Elevation of Östrand road bridge, originally produced by Skanska.

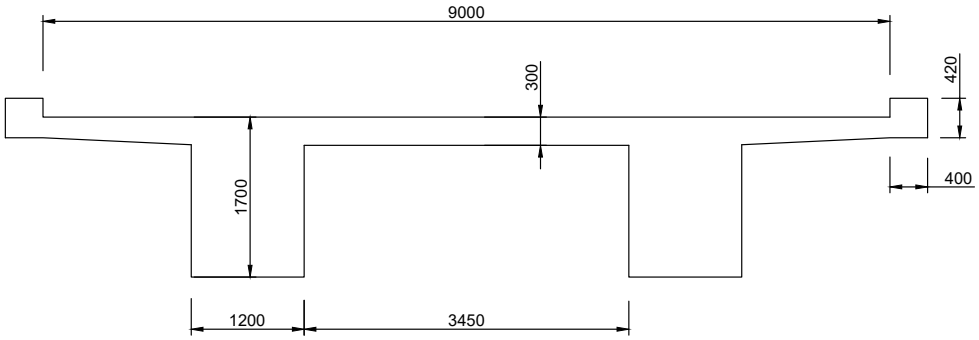

Figure 3.2: Cross-section of Östrand road bridge, with measurements in mm.

3.2 Modeling the reference bridge

The geometry of the reference bridge was modeled in the FE program BRIGADE/Plus to verify the structural behavior of the model to the original calculation report by Skanska, where *fem3dyn* was used as the FE solver. BRIGADE/Plus is further described in Appendix A. Total reactions, cross-sectional forces, and deflection were compared with the original results, both with self-weight and traffic loads applied to the bridge model, for verification, see Appendix B.

The system model in BRIGADE/Plus consists of beam and shell elements. The main beams, cross beams, and edge beams were modeled as wire elements with beam sections. To simulate the main beams' capacity to support the bridge in ULS, the bridge deck slab was modeled as a planar shell element with limited stiffness in the longitudinal direction, adjusted through the material property. However, to obtain the value of the deflection in SLS, the shell element of the bridge deck was modeled with an isotropic material. These assumptions were also made in the original calculations of the reference project.

The slabs and beams were connected by ties and couplings to represent "stiff-beam connections" or casted concrete connections. Couplings were used in node-node connections between the cross beam end nodes and the main beams. Ties connected the main beams to the slab surfaces above the beams. A view of the FE model is presented in Figure 3.3

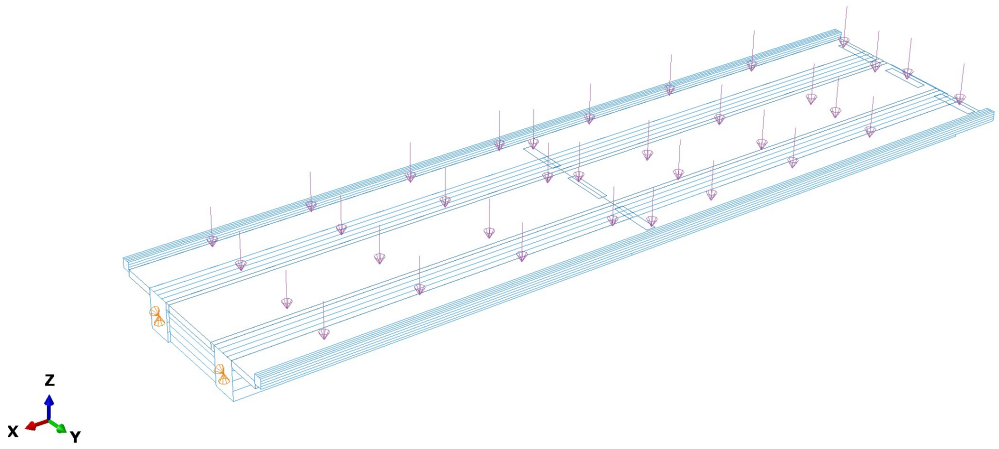

Figure 3.3: Sketch of structural model in BRIGADE/Plus, with distributed load and boundary conditions.

The original design of the Östrand bridge was made according to the regulations *Bro 2004* from the Swedish Transport Administration (Vägverket, 2004). To verify the FE model, traffic loads were applied to the bridge according to the same regulations. When continuing with the optimization algorithm, the traffic load was applied according to current standards and codes; see Section 4.2.

3.3 Modifications

Several modifications were made when modeling the reference project to simplify the process and minimize computational time. These adjustments include modeling the bridge straight, instead of curved with a radius of 100 m, and without inclination in any direction. The six point loads, placed in longitudinal and transversal directions on the bridge deck to simulate axial loading from traffic, according to Bro 2004 (Vägverket, 2004), were simplified by an equivalent transverse line load. In addition, the prestressing of the main beams was excluded from the model. Comparison with the results of the reference project verified all mentioned modifications; see Appendix B.

4

Applying the Set-Based Design Algorithm

The set-based design algorithm used in the study was coded in Python and consisted of three main parts: generations of design set, resistance verification, and multi-criteria evaluation. Figure 4.1 illustrates an overview of the algorithm layout, while Sections 4.1-4.3 give an in-depth description of each part.

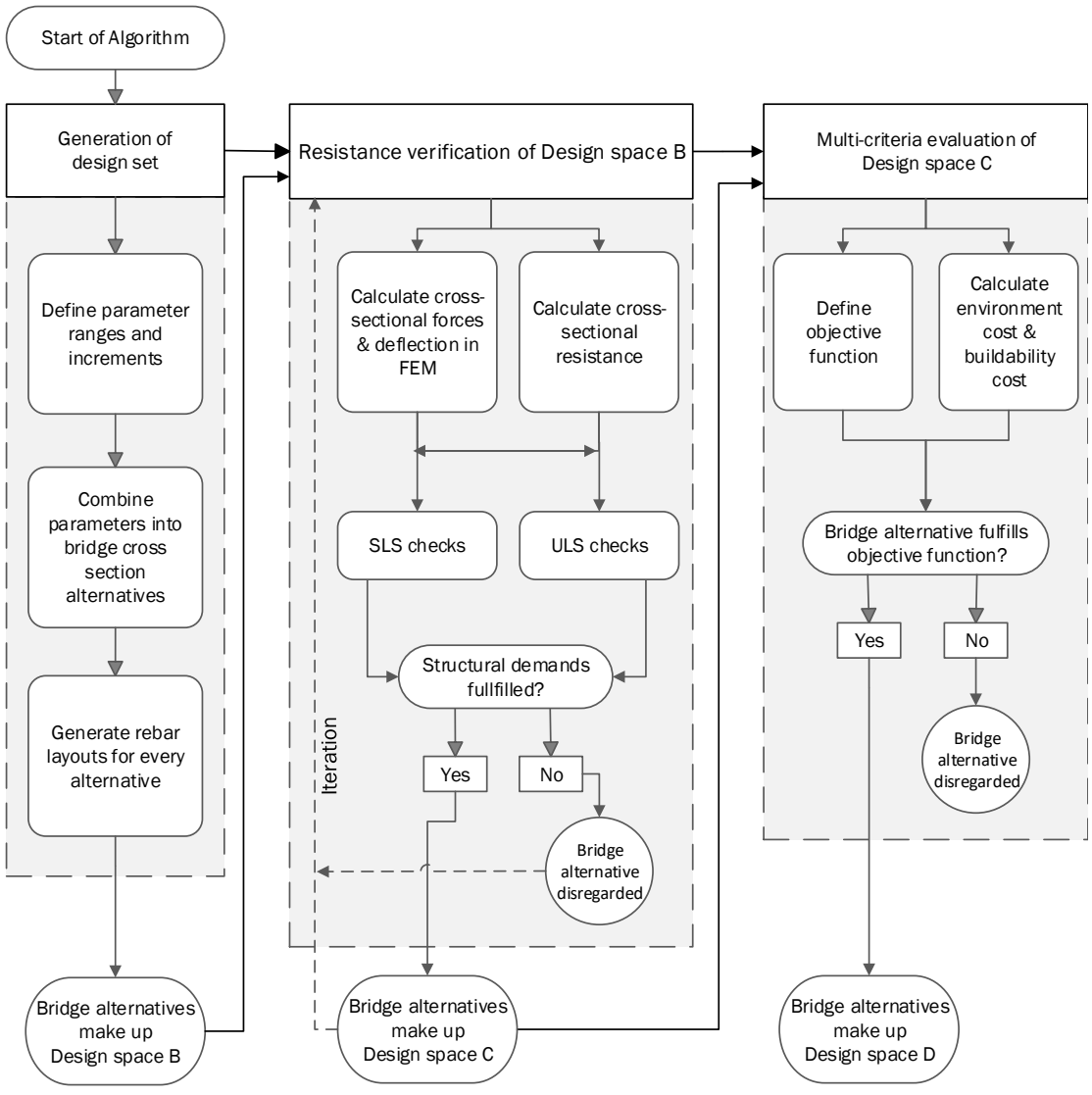

Figure 4.1: Layout of the SBD algorithm.

4.1 Generation of design set

The geometry of the bridge of the reference project acted as a basis for the generation of the design set. Some aspects of the bridge were chosen as fixed parameters, such as the span length, width and thickness of the bridge deck, thus making the girders the main focus in the cross-section variations. These parameters were considered to be the established governing geometry and, as a result, narrow down the Design Space A to Design Space B. The fixed parameters and their values are presented in Table 4.1.

Table 4.1: Fixed design parameters of girder bridge.

Fixed design parameter	**Value [m]**
Span length	35.5
Thickness of bridge deck	0.3
Width of bridge deck	9.0
Geometry of edge beams	0.4×0.42

The generation of Design Space B focused on two types of cross-sections, one with rectangular girders and one with I-profile girders. The intervals of the variable parameters were derived from the existing geometry of the reference bridge girders, including the design of the reference project within the selected ranges. The studied design parameters and their ranges for rectangular beam cross-sections are presented in Table 4.2.

Table 4.2: Parameter ranges and values for girder bridge cross-sections with rectangular main beams.

Studied design parameter	**Values**
Concrete strength class	C32/40, C35/45, C50/60
Reinforcement diameter	ϕ16, ϕ20, ϕ25 [mm]
Height of main beam	1.4, 1.5, 1.6, 1.7, 1.8, 1.9, 2.0, 2.1, 2.2, 2.3, 2.4 [m]
Width of main beam	0.8, 0.9, 1.0, 1.1,1.2, 1.3, 1.4, 1.5, 1.6, 1.7, 1.8 [m]

For I-profile beam sections, additional parameters studied were bottom flange thickness and web thickness. The width of the main beam of the rectangular girder was used for the width of both the top and bottom flange of the I-profile. The top flange was considered part of the slab and therefore had fixed geometry in terms of thickness. The bottom flange thickness and web thickness parameters were implemented in relationship with the beam height and beam width, respectively, as a ratio. This implementation was made to avoid the absurd randomized combinations that would otherwise occur with independent ranges. The chosen ratio intervals of the parameters of the I-profile are presented in Table 4.3. All parameters are also visualized in Figure 4.2.

Table 4.3: Additional parameter ranges for I-girder cross-sections.

Studied design parameter	Ratio range [m/m]
Web thickness	[0.30, 0.40, 0.50, 0.60, 0.70]
Bottom flange thickness	[0.30, 0.40, 0.50, 0.60, 0.70]

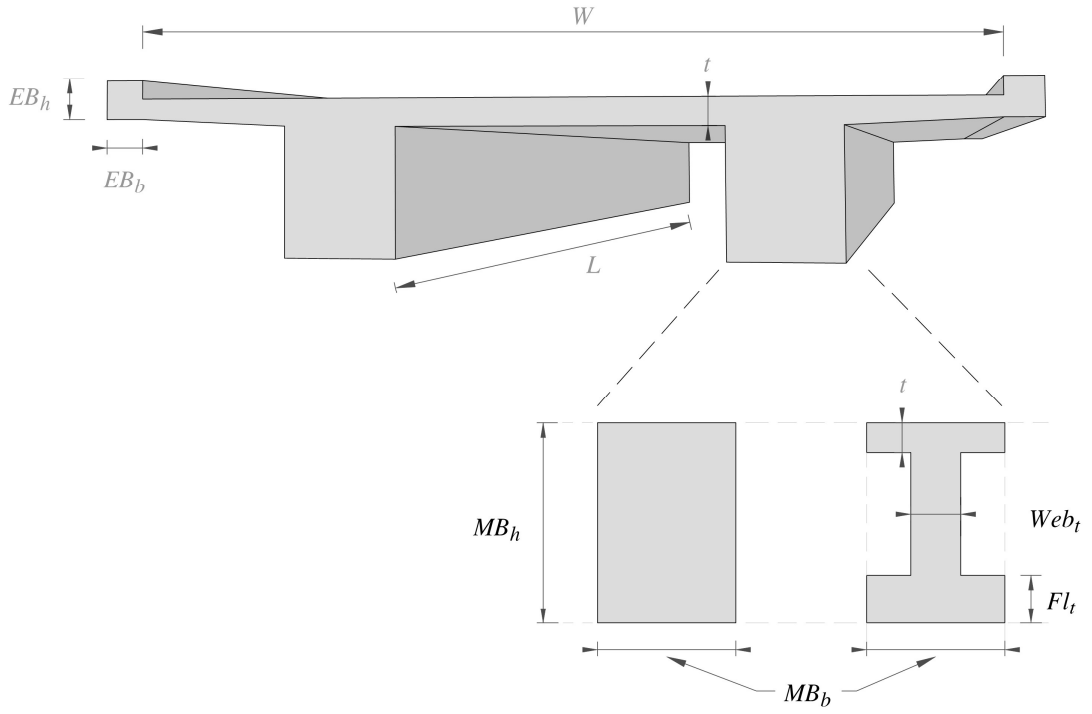

Figure 4.2: Bridge geometry width parameters illustrated. Fixed parameters are marked in grey and variable in black.

4.1.1 Rebar layout generation

For each concrete cross-section geometry, multiple tensile reinforcement layouts were generated for the beams, as part of a sub-algorithm in the script. The rebar layouts were created based on input from the beam geometry parameters, such as the necessary concrete cover, the width of the rectangular girder and the width of the I-girder flange, combined with a calculated required reinforcement amount A_s [mm^2/m]. To account for the curtailment of the reinforcing bars, the required reinforcement was determined at seven positions along the length of the bridge. These seven positions were also used when assessing the need and spacing for shear reinforcement. This level of detail was assumed sufficient for the calculation. If the same method were applied to a bridge with a shorter span, fewer evaluation points might be necessary, and vice versa. Figure 4.3 illustrates the sections in which the need for reinforcement was calculated.

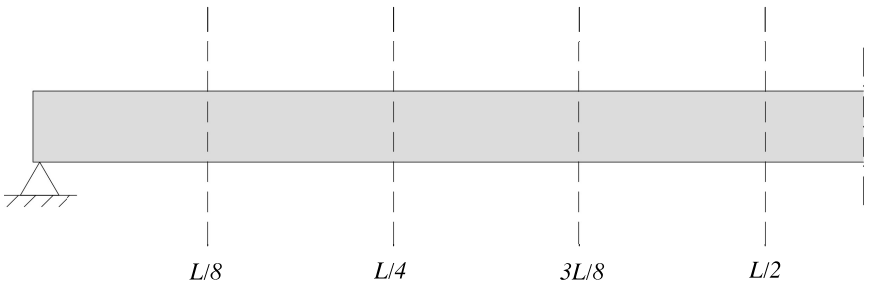

Figure 4.3: Assessment positions along the bridge, with example spacing of shear reinforcement.

At each position along the span, the algorithm assigned the required number of rebars to a layout according to common practice rules. The rules applied for longitudinal rebar placement were as follows:

- The bottom rebar layer is filled with the maximum number of bars possible before filling any additional layers.
- Rebar positions are stacked vertically to accommodate casting.
- The flange of I-section girders are filled with bars before placing bars in the web
- The uppermost layer of reinforcement always has an even number of bars for simplification.

The sub-algorithm takes concrete cover, rebar diameter and minimum spacing between bars, both vertically and horizontally, into account. Figure 4.4 presents the parameters incorporated in the algorithm, of which ϕ_{rebar} and f_{ck} were variable parameters from the input. f_{ck} was the characteristic strength in compression, dependent on the concrete class parameter. n_{layers} and n_{bars} refer to the number of layers of tensile reinforcement and the number of bars in each layer. These parameters were not part of the input but rather an output produced by the sub-algorithm, used in later steps to verify the capacity of each solution. A new rebar layout was created for each size of rebar diameter. Some variation in required reinforcement amount A_s was also introduced, to further widen the design space of possible reinforced concrete cross-sections. Relevant data from each rebar layout generated in this step was extracted to be used in the succeeding parts of the algorithm, namely the cross-section resistance verification in Section 4.2, and the multi-criteria evaluation in Section 4.3.

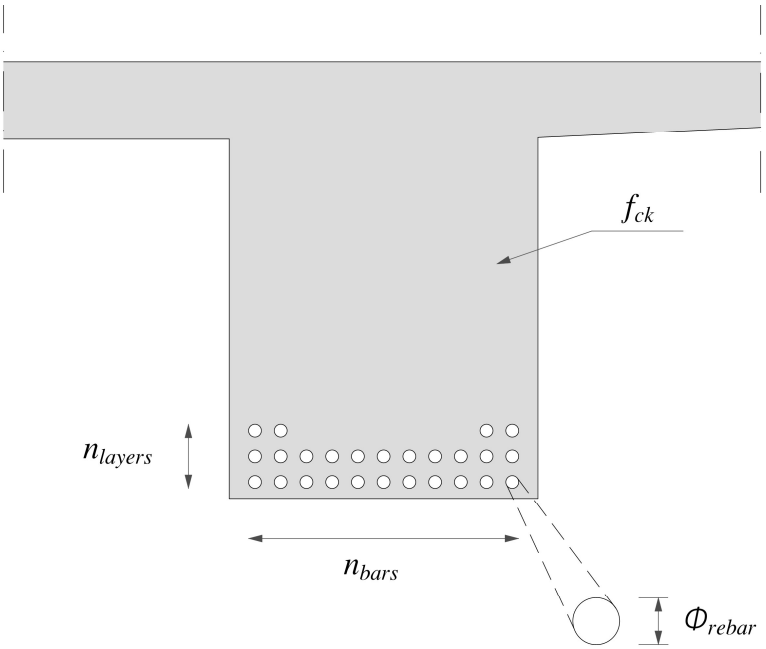

Figure 4.4: Parameters related to tensile reinforcement layout.

4.2 Resistance verification

The second part of the set-based design algorithm was the verification of the structural resistance of Design Space B. This includes the use of FEM to analyze the load effects on the structure, with the applied loads and load combinations presented in Sections 4.2.1-4.2.2. The structural verification in ULS and SLS is described in more detail in Section 4.2.3. Figure 4.5 shows an overview of the structural verification process, narrowing down Design Space B to a smaller Design Space C, which contains only feasible solutions.

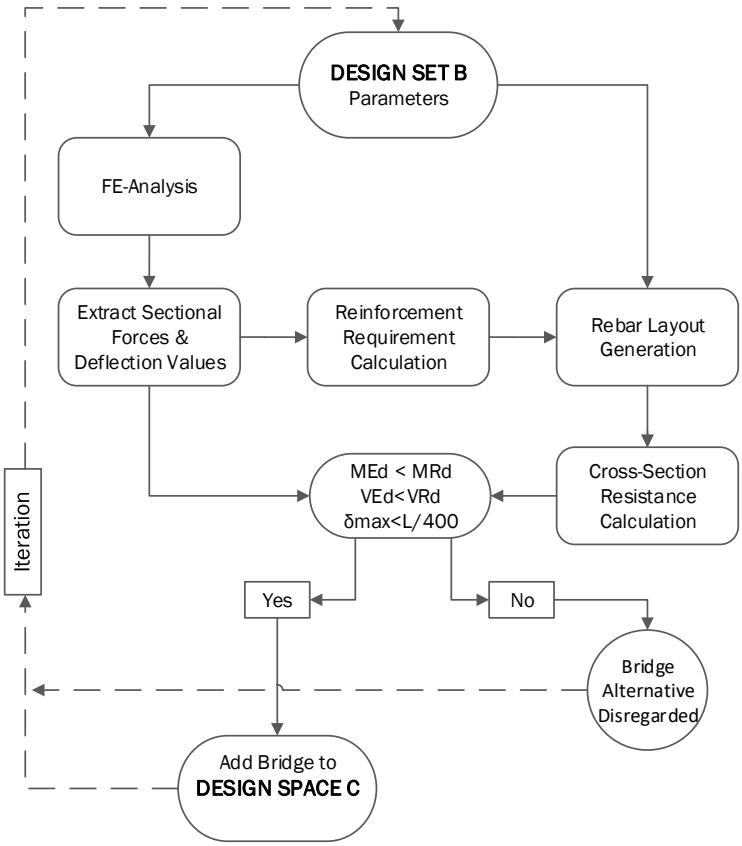

Figure 4.5: Verification algorithm layout

4.2.1 Load categories

Both permanent and variable loads are applied to the bridge in the FE-model for structural verification. Further descriptions and calculations of the loads applied are found in Appendix C.

Permanent loads include:

- Self weight
- Pavement

The variable loads include:

- Traffic load
- Braking forces
- Side forces

Self-weight was applied as gravity load for all concrete elements in the FE model, while the pavement load was modeled as a uniformly distributed pressure over the bridge's road surface. The traffic load was applied according to LM1 in SS-EN 1991-2 (Swedish Institute for Standards, 2011) and, as described in Section 2.6, consists of concentrated and uniformly distributed loads. The national vehicle model was not used in this case as it was not considered governing. Braking forces, with its transverse component as

side forces, were modeled as surface traction forces in one lane. Wind load was not considered as the bridge did not have a sufficient height for it to be necessary.

The positions of the traffic axle loads were manually adjusted instead of using the built-in function in BRIGADE/Plus, to aid in computing time. The shear force was analyzed with the concentrated load positioned near the supports and the moment and deflection when it was placed at mid-span.

4.2.2 Load combinations

For verification in ULS, load combination *Bb Method 2* was used according to SS-EN 1990 (Swedish Institute for Standards, 2010), where the variable load is dominant rather than the permanent load. The distributed part of the traffic load was chosen as the main load. In SLS, the frequent values of loads are used. The distributed part of the traffic load was also chosen as the main variable load in this analysis. The deflection limit was set to $L/400$, with L being the theoretical span length.

4.2.3 Structural verification in ULS and SLS

According to SS-EN 1990 (Swedish Institute for Standards, 2010), there are several performance requirements to satisfy for newly constructed concrete bridges. These demands include the ultimate limit state (ULS), service limit state (SLS), as well as the fatigue limit state (FLS), according to SS-EN 1991-2 (Swedish Institute for Standards, 2011). ULS considers the maximum resistance of the structure until the point it reaches failure. The design loads determine the resistance of the structure in ULS. Although designing for ULS prevents structural failure, SLS requirements ensure functionality for the entire service life of a structure. Thereby, demands limiting cracking, deformations, and vibrations are accounted for in SLS design. FLS regards the cyclical load that bridges with train or road traffic are exposed to. Following the limitations of this thesis, FLS verifications are excluded from the calculations.

The structural analysis was performed according to Eurocodes with national amendments, accounting for the bending moment and the shear force in the ultimate limit state and deflection control in the serviceability limit state. Long-term effects were excluded. The demands applied to the structure are shown in Table 4.4. The design constraints for ULS were checked in the assessment positions marked in Figure 4.3, while for the SLS and deflection it was only checked in the mid-span. To further limit the complexity of the structural verifications, the ULS and SLS checks were only performed along the length of the bridge, load effects in the transverse direction were excluded.

Table 4.4: Design constraints applied to Design Space B.

Design constraints		**Definition**
Ultimate limit state (ULS)	Bending resistance	$M_{Ed} - M_{Rd} \leq 0$
	Shear resistance	$V_{Ed} - V_{Rd} \leq 0$
Serviceability limit state (SLS)	Deflection	$\delta_{max} - L/400 \leq 0$

To find the design values M_{Ed} and V_{Ed}, as well as the maximum deflection δ_{max}, FE analysis was performed. The FE program BRIGADE/Plus was chosen for the analysis

mainly because of the possibility of parameterizing a Python script to run the program, enabling iterative processing of all bridge solutions in Design Space B. The structural analysis was limited to linear elasticity to minimize computational complexity, which is considered sufficient for the initial design phase. The relevant sectional forces in the girders, which were the shear force and the bending moment in the chosen sections of the bridge, as well as vertical deflection in the mid-span, were extracted from the output database and saved to a results file for verification.

The bending moment resistance M_{Rd} of each cross section, considering the rebar layout generated for each cross section, and the shear resistance V_{Rd}, and thus the need for shear reinforcement, was calculated as in Appendix D. The verification part of the algorithm script took the result files from the FE analysis and compared the sectional forces to the calculated cross-sectional resistance for each bridge in the design set. It also compared the deflection value with its limit of $L/400$. Any bridge solution that meets these criteria was added to Design Space C.

4.3 Multi-criteria evaluation

The final stage of the algorithm further evaluated the feasible design range, Design Space C, against three criteria: investment cost, environmental impact, and buildability. The investment cost included both material and labor costs; the calculation is presented in Appendix E.2. To enable a comparison between the different criteria, the level of buildability and environmental impact was converted into monetary cost, hence an environmental impact cost and a buildability cost were calculated. Formwork was cut-off in the calculated cost for both buildability and environmental impact. Based on the criteria costs, the lowest 10% of bridge alternatives in Design Space C were included in Design Space D.

The environmental impact cost was calculated from the steel and concrete volumes used for each bridge. The Ecovalue12 monetary weighting system was chosen to calculate the environmental cost as it was considered the most relevant for this application and was the most recent version available. The calculations in detail can be found in Appendix E.1.

For the I-beam sections, additional volume was added to account for a 45 degree incline between the flanges and the web, needed to accommodate casting. This added area was not included in the structural analysis of the bridge cross-section, but solely to adequately represent the volume of the bridge in terms of material cost and CO_2 emissions.

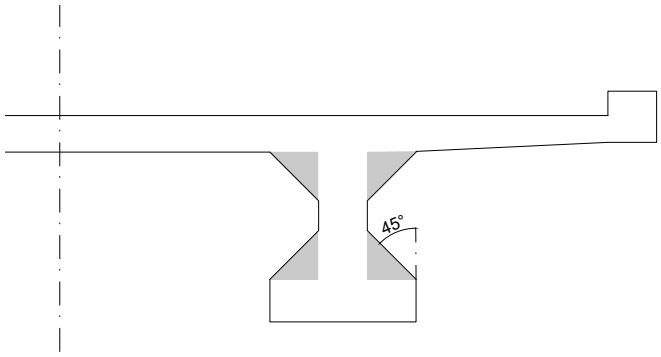

Figure 4.6: I-girder bridge cross-section with inclined part of flanges marked.

The calculated volume of reinforcement included the anchorage length for all three criteria. For tensile reinforcement, anchorage length was considered as an additional rebar length of 50ϕ. For shear reinforcement, 10ϕ accounts for the length of one hook in stirrups with standard hooks.

Based on the theory presented in Section 2.5.2, the buildability criteria chosen as relevant for this study were:

- reinforcement diameter,
- slender element parts,
- use of shear reinforcement,
- concrete class, and
- shape of girder.

The calculation procedure for the buildability cost is presented in Appendix E.3. To simplify FE modeling, all elements parts were modeled with constant thicknesses. Consequently, the buildability criterion related to varying thickness was excluded from this study. Among the remaining criteria, the one regarding the slender elements affects all bridges due to the slenderness of the bridge deck. However, it is particularly relevant for the I-sections, which may contain thinner webs or flanges that affect both buildability and resource efficiency.

The buildability of the I-girders was assumed to be less than that of the rectangular girders. Given the span length of the studied bridge, the girders of concrete I-sections and rectangular sections would probably be casted in situ. This aspect reduces the buildability of the I-section compared to the rectangular beam sections. In consultation with an experienced construction engineer at Skanska, it was estimated that I-girders casted in situ have a 50% longer labor time for reinforcement work than for rectangular girders, equivalent to an increase in the reinforcement labor cost of 50%. This was implemented as a factor in the calculation of buildability cost, see Appendix E.3. However, if the span length was shorter, less than 12 meters and fitting on a standard truck, it could have been pre-fabricated. Including the aspect of prefabrication would instead increase buildability compared to any girder shape casted on site.

Thus, the investment cost, the environmental cost, and the buildability cost were obtained for all bridge alternatives in Design Space C. The sum of these three criteria

costs are henceforth referred to as the total cost. Alternatives in Design Space C that fell within 10% of the lowest values in each of the three criteria formed Design Space D. The definition of Design Space D marked the final step of the optimization algorithm and concluded the methodology. The subsequent chapter presents the results of the comparative analysis of the design alternatives of Design Spaces B, C and D.

5

Results

The algorithm, described in Chapter 4, was run with the given input parameters. The running time was 50 hours for the generation and FE-analysis part of the script and approximately 10 minutes for the post-processing of the FE-results, including structural verification and evaluation based on the chosen criteria. The resulting number of bridge alternatives in each design space can be found in Table 5.1.

Table 5.1: Size of data set in each design space.

Design space	**Nr. of designs in set**
Design Space B	113 256
Design Space C	69 025
Design Space D	6 902

5.1 Mapping of design spaces

To accommodate the comparison between the design alternatives and the design spaces, output values of CO_2 emissions, buildability cost, and investment cost were normalized according to the smallest value, making it equal to 1.0 and the remaining values as factors thereof. The probability density curves, overlaying histograms are shown in Figures 5.1-5.3 for the three criteria studied.

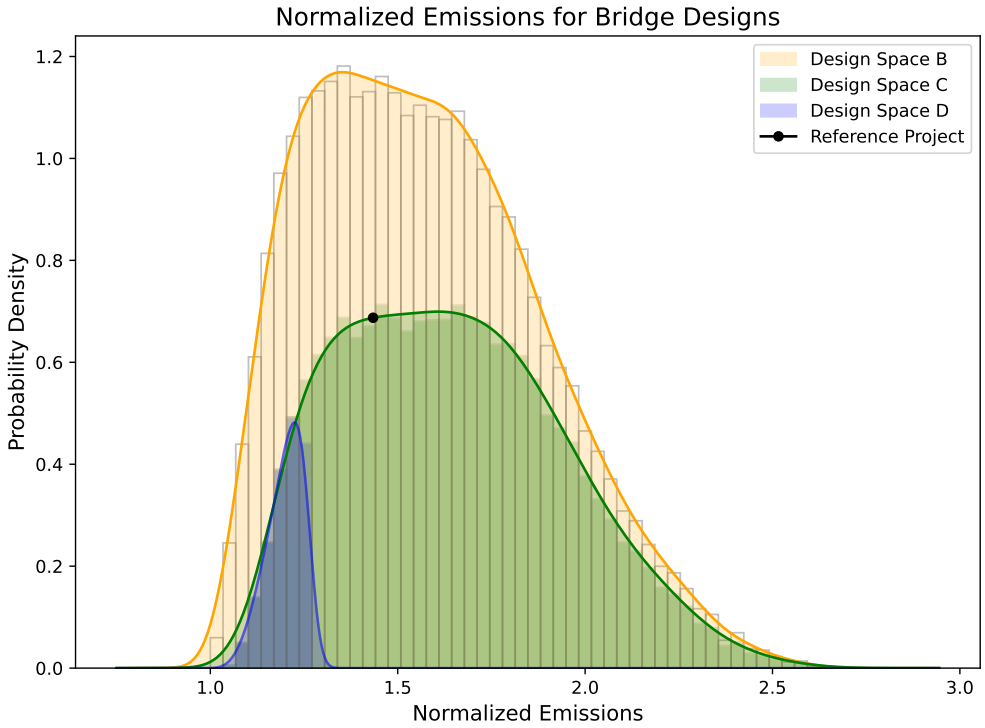

Figure 5.1: Normalized emission distribution of bridge alternatives.

As Figure 5.1 shows, Design Space C is contained within Design Space B and slightly shifted towards the right. This shift suggests that the feasible designs on average require more material than the average of the group of infeasible designs. It also suggests that Design Space B and the chosen ranges of design parameters cover all feasible solutions with the lowest CO_2 emissions. The probability function somewhat follows a normal distribution, meaning that very few of the alternatives have significantly lower climate impact than most of the alternatives. Design Space D is contained within Design Space C and located to the left as it consists of feasible bridge solutions with the lowest 10% of emissions. The reference project is located approximately at the center of Design Space B, in terms of normalized CO_2 emissions. There being about the same amount of bridge alternatives with lower and higher emissions respectively, compared to the reference is a result of the reference being used as a base for the design generation.

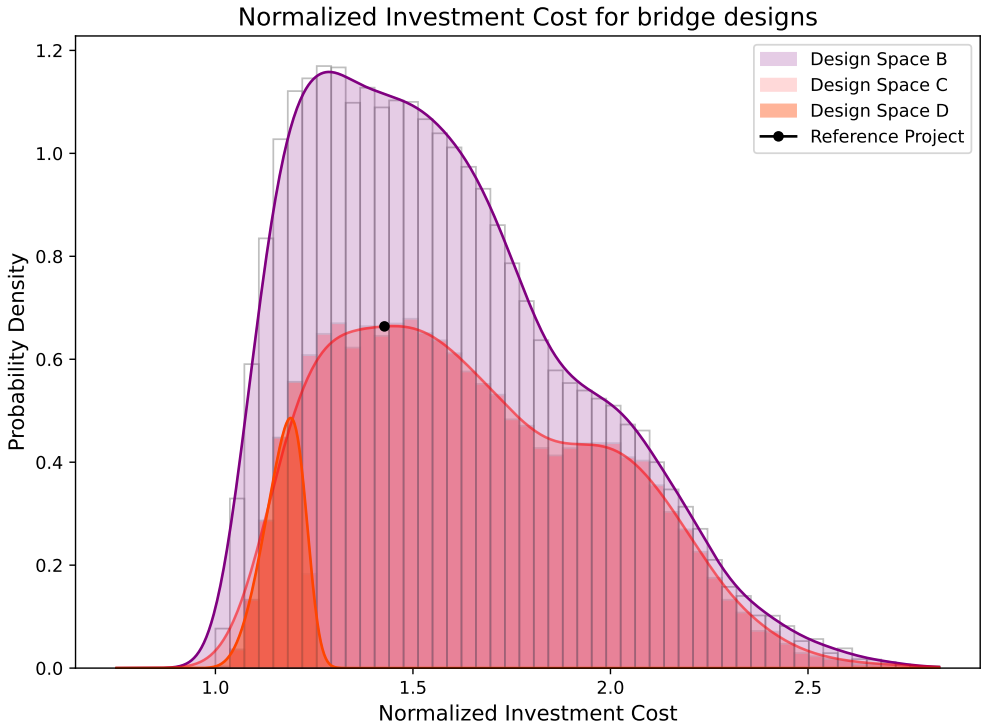

Figure 5.2: Normalized investment cost distribution of bridge alternatives.

In Figure 5.2, it is clear that the probability function of the investment cost distribution does not follow a normal distribution, but rather a bimodal one. This implies that two or more distributions with different characteristics are combined, which is the case in this study, as multiple parameters are varied between alternatives in the generated design space. Design Space C mirrors the distribution of Design Space B, with the reference project centrally displayed in the first mode. In addition, Design Space C is slightly shifted towards the right inside Design Space B, suggesting that the chosen ranges of design parameters cover all feasible solutions with the lowest investment cost.

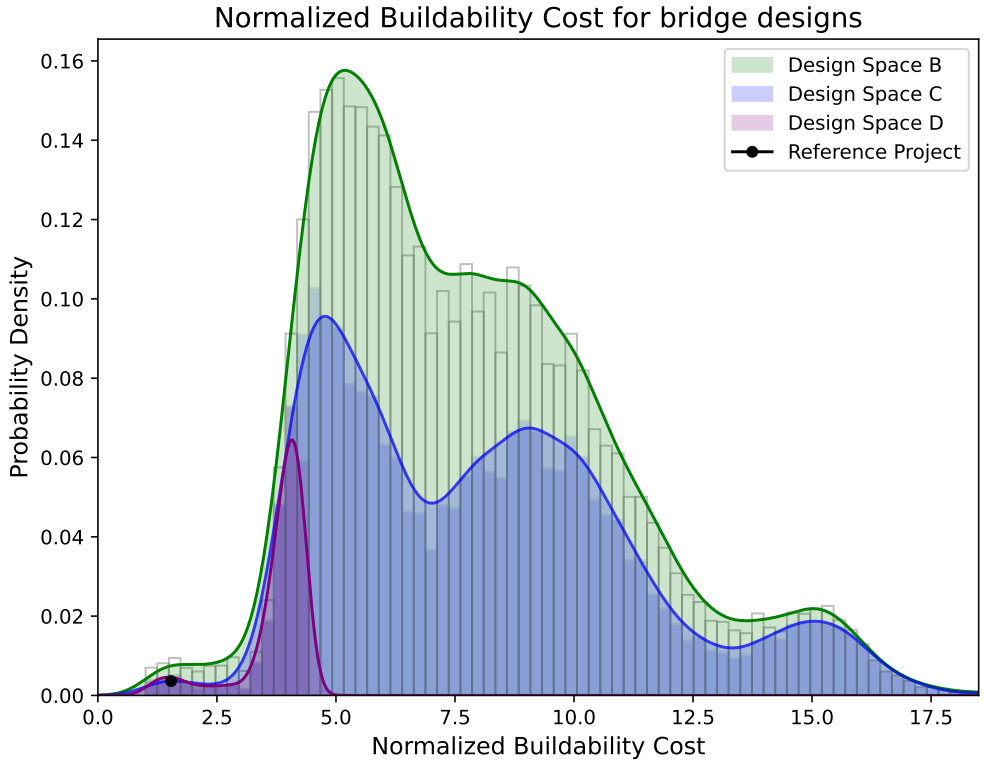

Figure 5.3: Normalized buildability cost distribution of bridge alternatives.

The probability density function that displays the normalized buildability cost in Figure 5.3 differs from the previous two functions, in the sense that it more clearly exhibits a multi-modal distribution. This appearance exists because the objective function related to the buildability criteria is evaluated through a number of combined discrete functions, see Appendix E.3. The difference in scale between the distributions of the different criteria is also notable, with the normalized buildability cost spanning up to 17.5 times that of the lowest in the range, whereas the other two criteria have a more concentrated distribution. Section 6.2 expands on these differences. The reference project is located in the first small local maxima, meaning that it has a lower buildability cost than the vast majority of solutions through all design spaces.

5.2 Relationship between criteria

The representations of the design spaces in Section 5.1 illustrate how each evaluation parameter is distributed independently within the space. However, examining these parameters in isolation does not capture the relationships and trade-offs between them. To gain a more comprehensive understanding of the feasible design space, it is essential to analyze how the evaluation parameters interact with and influence each other. Thus, this section focuses on the comparative relationships between the criteria, enabling a deeper exploration of Design Space C.

The relationships between the different criteria, investment cost, environmental cost, and buildability cost, are visualized using scatter plots. Additionally, the interrelationship of labor cost and material cost is presented in a similar manner. Figures 5.4-5.7 illustrate these results. To enhance clarity in the plots, only one in every 50 bridge alternatives are shown.

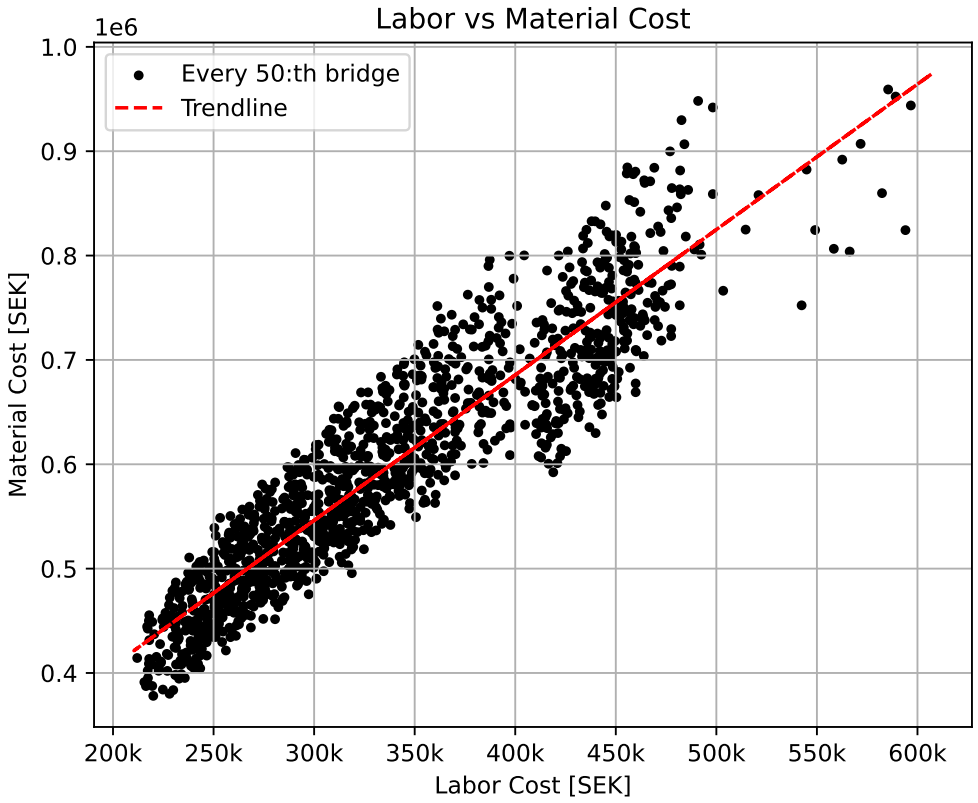

Figure 5.4: Relationship between labor and material cost.

The relationship between labor cost and material cost, the two components that make up the investment cost in this report, is shown in Figure 5.4. The linear relationship observed is strong, with some disparity around the trend line. This relationship is explained by the dependence on material amounts for both labor cost and material cost to be calculated.

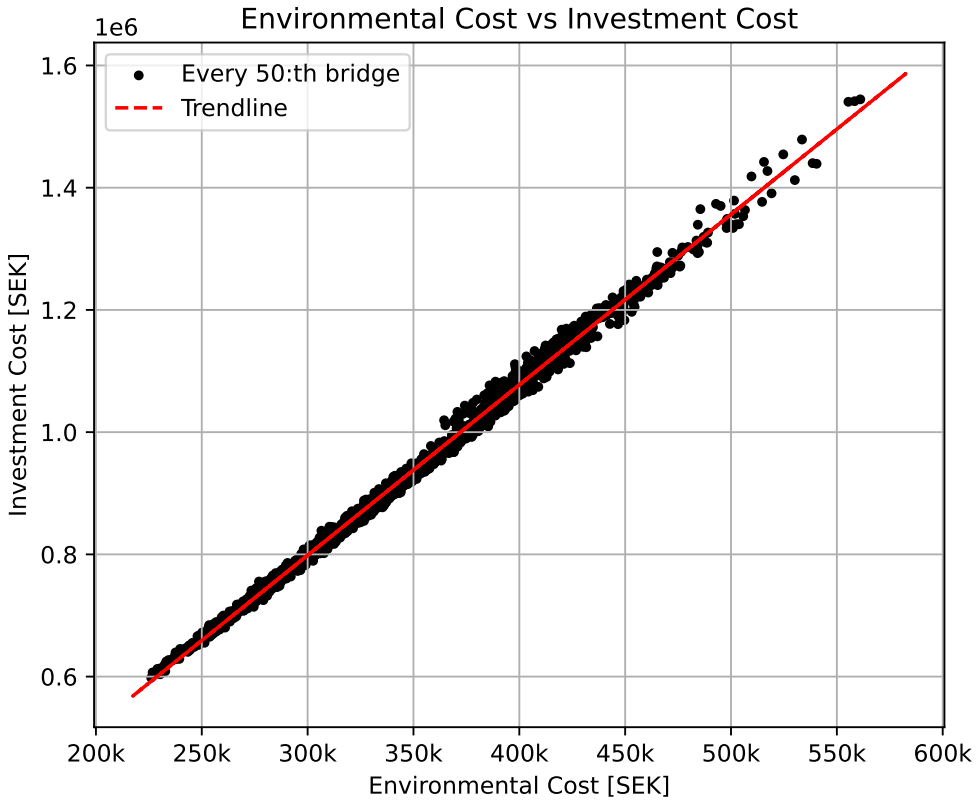

Figure 5.5: Relationship between investment cost and environmental cost.

A clear linear correlation between investment cost and environmental cost is visible in Figure 5.5. This is probably due to the dependence on material quantities in both cost functions, as both investment cost and environmental impact are heavily influenced by the volumes of steel and concrete used in the bridge construction. The near perfect linearity of the plotted data indicates that environmental and investment costs scale almost proportionally between design alternatives. This suggests that, in this dataset, it is difficult to reduce one without also reducing the other, highlighting a strong coupling between economic and environmental performance. In practical terms, more material-intensive designs lead to both higher monetary costs and higher CO_2 emissions.

The data points in Figure 5.5 exhibit minimal scatter around the trend line, compared to the other parameter relationships, see Figures 5.6-5.7. This implies a high level of predictability between the two parameters, which could simplify early-stage decision-making or optimization when one parameter is prioritized.

Furthermore, the consistency of the data across the entire range of values suggests that no particular subset of designs significantly deviates from this relationship. This observation supports the interpretation that material efficiency is a critical driver for both investment and environmental performance in bridge design.

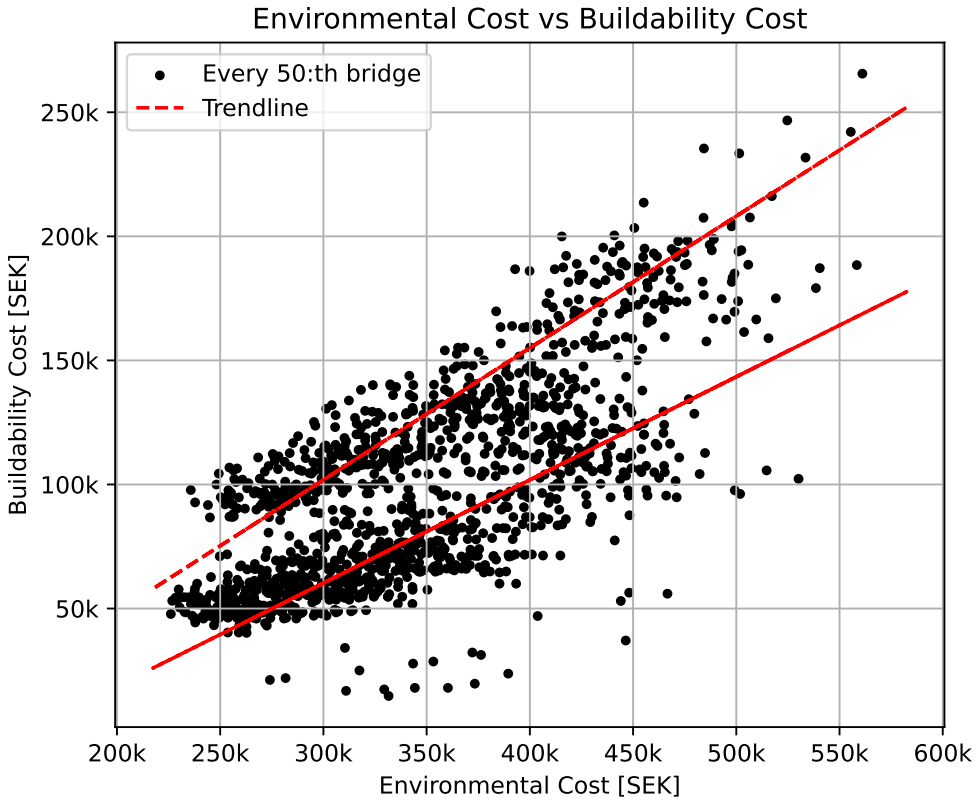

Figure 5.6: Relationship between buildability cost and environmental cost.

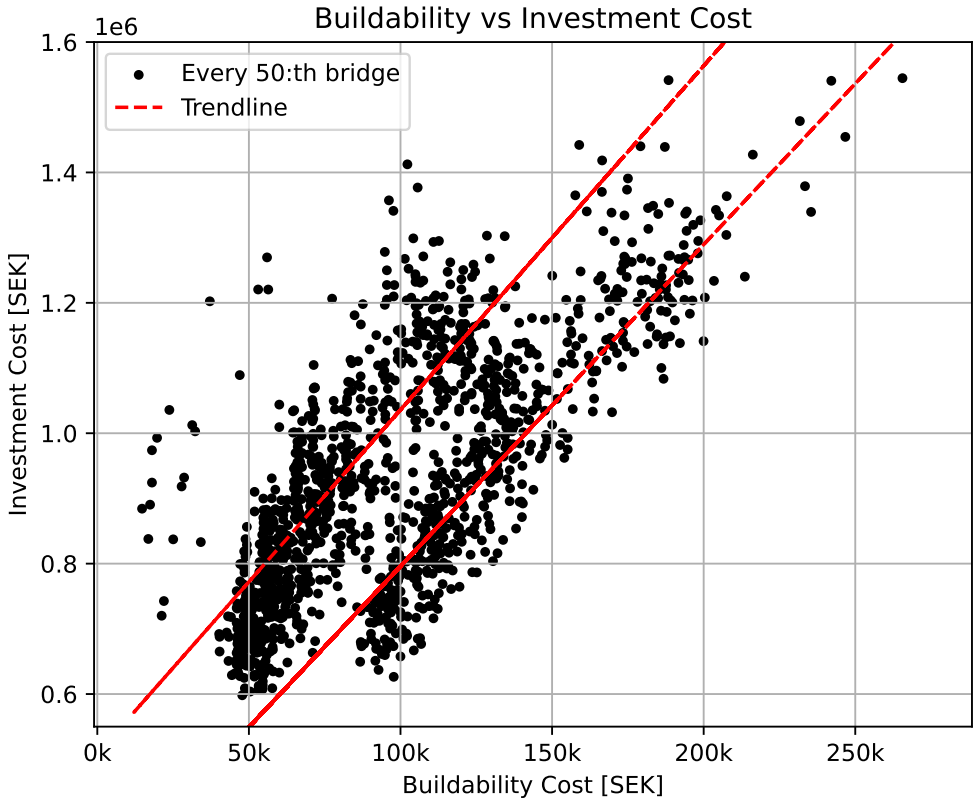

Figure 5.7: Relationship between investment cost and buildability cost.

The scatter plot in 5.6 reveals a positive correlation between environmental cost and buildability cost; as environmental cost increases, the buildability cost tends to increase as well. This suggests that designs that are more environmentally costly also tend to be more complex and expensive to construct. However, there is noticeable dispersion around the trend line, indicating variability in the relationship. Some designs exhibit relatively low buildability costs despite high environmental costs, and vice versa.

In Figure 5.7, there is also a positive linear relationship, but between the investment cost and the buildability cost. Bridge alternatives that are more complex to construct also have a higher initial investment cost, but the deviation from this interrelationship is still prominent among the data.

Furthermore, the data points in Figures 5.6 and 5.7 appear to form distinguishable clusters or subsets, suggesting a potential division within the design space. Hence, the application of two trend lines better fit the data than a single line would. This pattern being present in both figures illustrating buildability cost signifies the presence of the various discrete functions included in the buildability criterion, influencing the cost structures. Such a pattern warrants further investigation, as understanding these groupings could provide deeper insights into trade-offs and guide more targeted decision-making. Section 5.3 expands on this topic.

5.3 Comparison of sets within Design Space C

To gain a better understanding of how different subsets relate to the criteria in the feasible design space, the results are sorted according to different characteristics. In this section, the effects of main beam shape, concrete class, and rebar diameter are explored through colored scatter plots. The effects of the use of shear reinforcement as a buildability aspect was not considered to be of interest to investigate in the same way, as every bridge alternative needed shear reinforcement, just in different amounts. Although it was significant to the buildability cost, because the geometry of the design affected the amount of shear reinforcement, the criterion itself would not show anything being displayed by itself. In a similar way, the buildability aspect of slender cross-sections was estimated to effect only a small amount of the design set, and only I-shaped girders, and displaying only that in a plot seemed irrelevant. Thus, its effect is incorporated into exploration of the effect of the girder shape, increasing some of the I-girder's buildability cost.

5.3.1 Evaluation based on girder shape

When displaying the distributions of the two main girder shapes, the settings were adjusted to adequately display the spread of the rectangular alternatives in the plot. As the sample sizes of the two groups vary, with about 25 times more I-profile girders than rectangular girders in the data, the number of I-profile alternatives plotted was especially limited to achieve a readable result. Hence, Figure 5.8 does not reflect the actual sample sizes but rather shows the distribution of the two groups.

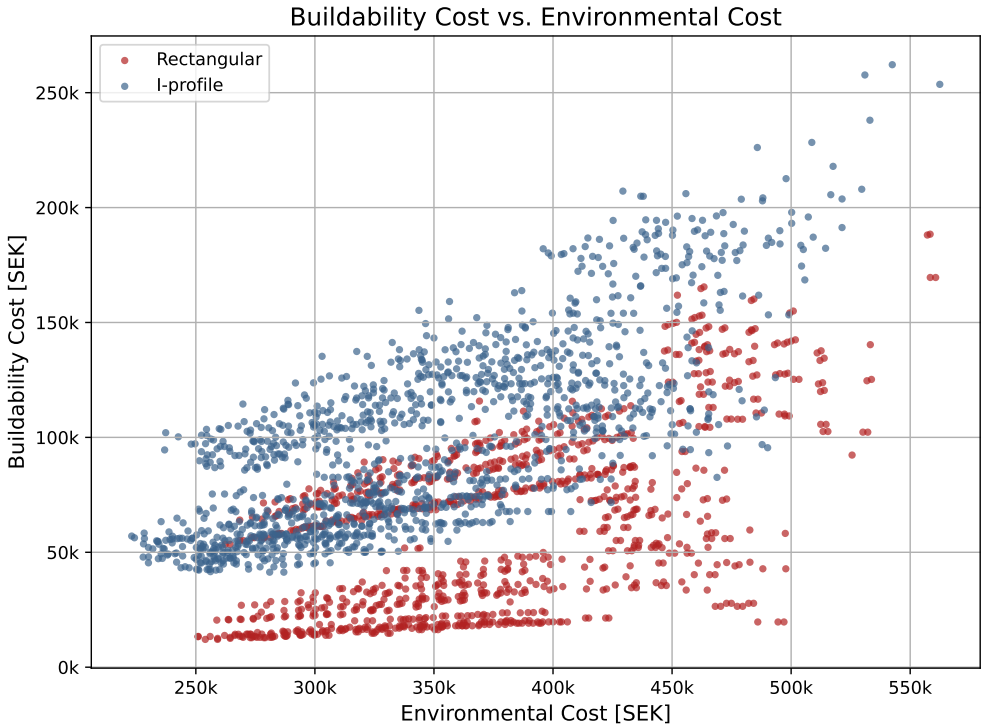

Figure 5.8: Buildability cost plotted against environmental cost for I-profile and rectangular girder bridge cross-sections respectively.

Visualizing how the two girder shape groups perform in terms of buildability cost and environmental cost in Figure 5.8, cross-sections with rectangular-shaped main beams tend to have a lower buildability cost but a slightly higher environmental cost than most of the I-profile girders. This could be explained by the increased material consumption of concrete in rectangular girders, which resolves the higher environmental impact, and thereby environmental cost, compared to I-girders. The lower buildability cost comes from a simpler construction process when casting rectangular girders. Although there is this visible distinction between the girder shapes, there is also a relatively large area where the two categories overlap; where the buildability cost and environmental cost are of equal magnitude for both cross-section types, showing that all I-sections do not automatically have higher buildability costs than rectangular girders.

5.3.2 Evaluation based on concrete class

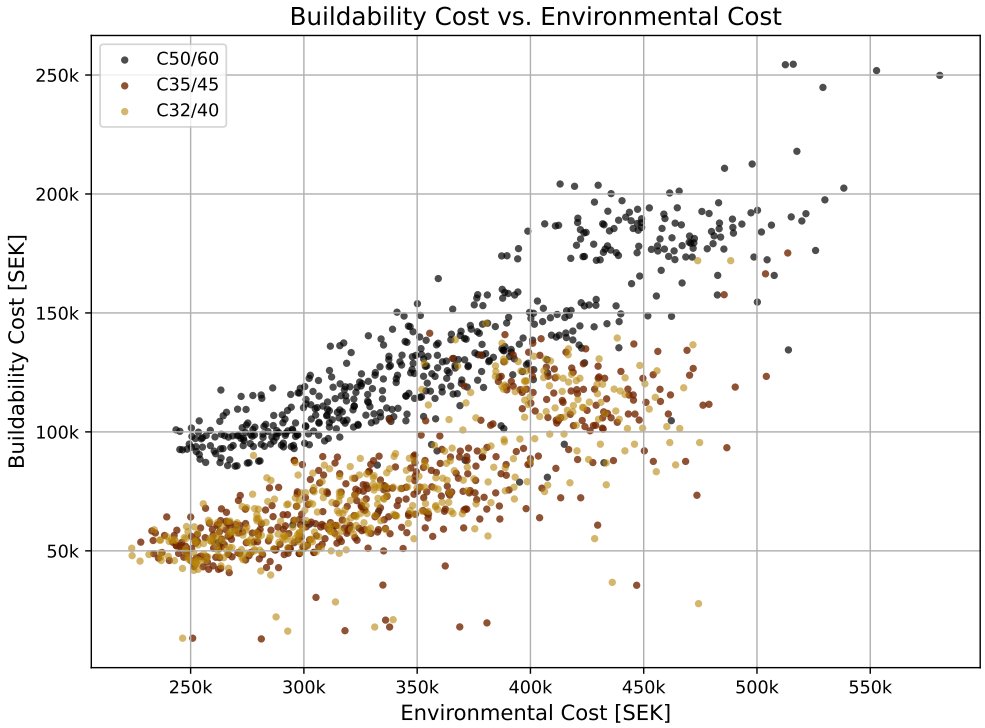

Figure 5.9: Buildability cost plotted against environmental cost for bridge alternatives with different concrete classes. 1 in 50 bridges plotted.

Regarding concrete class, it is apparent that sets of bridge alternatives with a higher concrete class give a higher buildability cost and a slightly higher environmental cost, as presented in Figure 5.9. There is a clear divide between the C50/60 class and the other two, class C35/45 and C32/40, suggesting concrete class has a big impact on the buildability cost. For the environmental impact, all concrete classes span over a large range considering environmental cost, but the alternatives with the least environmental cost consist of bridges using concrete class C32/40 or C35/45, and the alternatives with the very high environmental cost are predominately using C50/60.

5.3.3 Evaluation based on rebar diamater

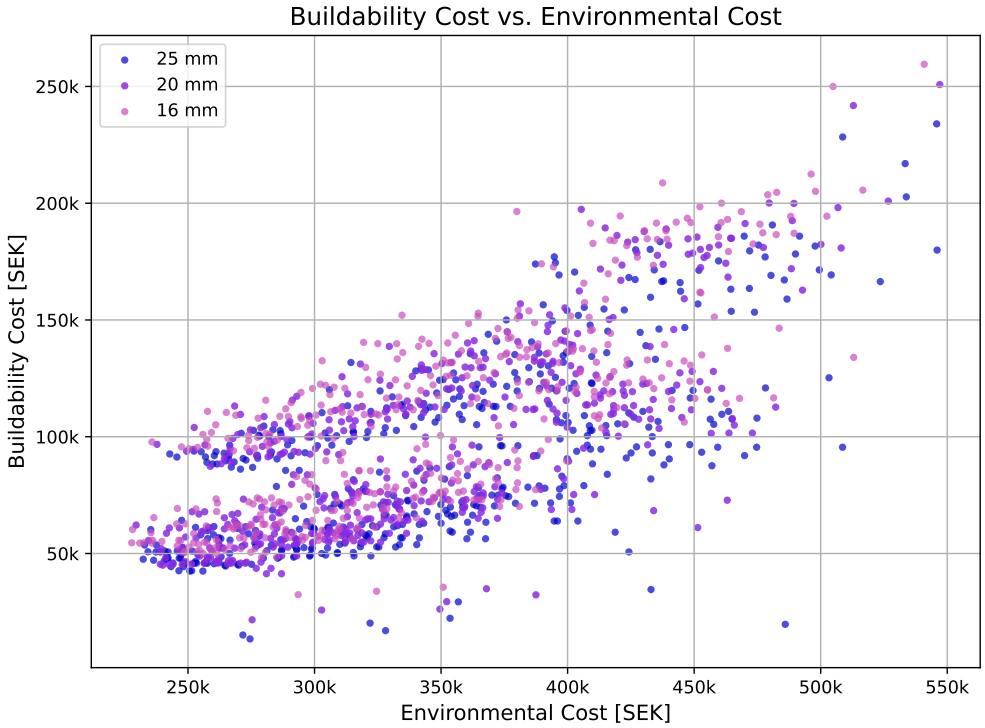

Figure 5.10: Buildability cost plotted against environmental cost for bridge alternatives with different rebar diameter. 1 in 50 bridges plotted.

Unlike the previous characteristics evaluated, the choice of rebar diameter does not show an obvious correlation with the clusters initially observed on Figures 5.6-5.7. As Figure 5.10 shows, bridge alternatives of all rebar diameters are spread somewhat evenly across the plot. This suggests that rebar diameter is not the determining factor in the buildability or environmental impact of a bridge alternative. However, there is trend in each cluster that a greater rebar diameter correlates with a lower buildability cost.

5.4 Exploration of Design Space D

In this section, the smaller feasible Design Space D, that is made up of the 10% of solutions with the lowest cost for each criteria, is explored further. As Section 5.3 showed, both girder shape and concrete class greatly impact both the environmental and buildability criteria, and thus the total cost. As solutions combining a high level of buildability with a low environmental impact are of particular interest in this study, Figure 5.11 displays the overlap in bridge alternatives between the lowest 10% of these two criteria costs.

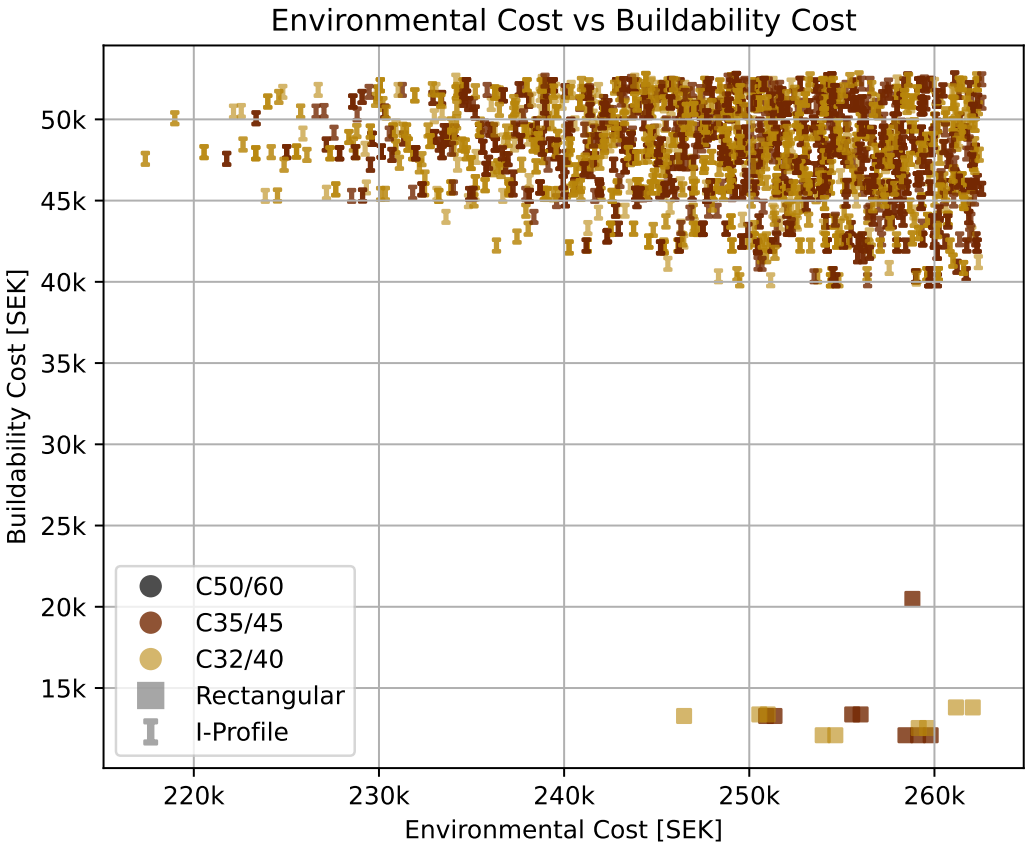

Figure 5.11: Relationship between buildability cost and environmental cost for the overlapping set in Design Space D, with the beam shape and concrete class presented for every solution.

The same pattern as previously found in Section 5.3 is clearly shown also in Figure 5.11, with only the lower concrete classes found in the alternatives in this set. There is a distinct divide between the two cross-section girder shapes, with the rectangular girder group performing better on buildability and the I-profile girders exceeding in environmental impact. The costs, however, seem to outweigh each other with a difference of about 35,000 SEK between the lowest cost for each criteria and shape. Meaning, the most buildable rectangular option costs ca 35,000 SEK more in environmental cost than the most resource efficient I-profile, which instead costs about the same amount more in terms of buildability cost. Hence, the total cost is valuable to observe, as it is the final cost for the client which is often the deciding factor. To further study the alternatives with the lowest costs, Figure 5.12 breaks down the total cost of the bridge alternatives of each type of girder which have the lowest emissions and buildability cost.

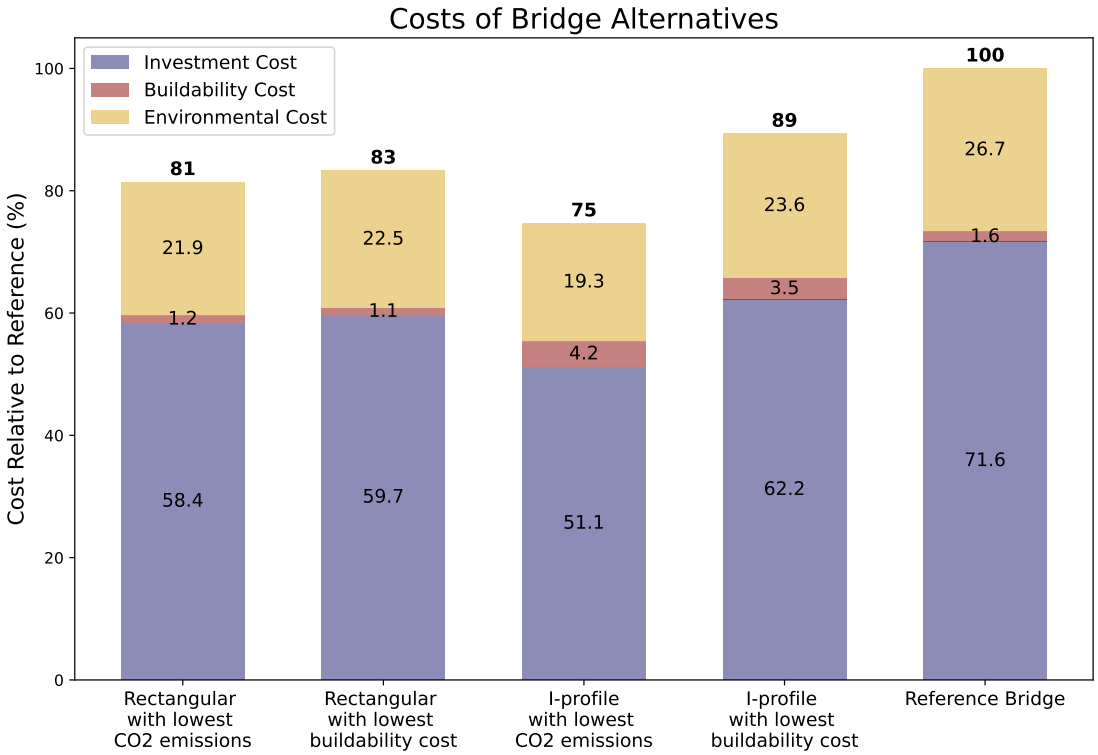

Figure 5.12: Total cost including the three criteria costs, for different bridge alternatives. Values relative the total cost of the reference project are displayed for each part.

As can be observed in Figure 5.12, the alternatives with the lowest CO_2 emissions for each of the two shapes studied are also those with the lowest investment cost and therefore the lowest total cost. This complies with the linear correlation presented in Figure 5.5. These solutions reduce the total cost by 19% and 25%, compared to the reference project. The bar diagram also shows that the buildability cost is not a major part of the total cost. An I-profile alternative has the lowest total cost, despite a noticeably higher buildability cost - almost four times as large - compared to options with rectangular girders. Thus, this comparison indicates that material efficiency may have a greater impact on total cost than the additional labor accounted for through the buildability cost. The geometry of the two bridges with the lowest total cost can be seen in Figure 5.13.

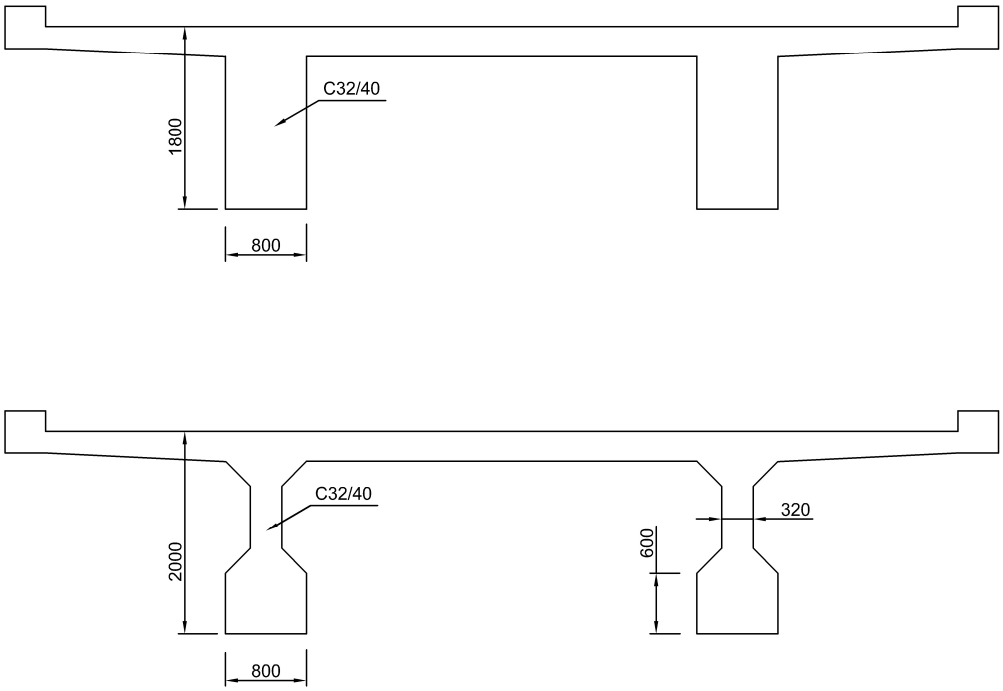

Figure 5.13: Geometry of the bridge cross-section alternative of each girder shape that have the lowest total cost. Measurements are presented in mm.

The bridge alternative with the lowest total cost for each shape shares some common variables, such as the main beam width of 800 mm, the concrete class C32/40, and the rebar diameter of 25 mm. However, the two options differ when it comes to beam height, with 1800 mm and 2000 mm, respectively, and the I-profile option has a slender web of 320 mm.

In summary, the results presented in this chapter reveal clear trends in the relationship between the criteria studied, alongside notable variations in data covering the buildability aspect. These findings provide a foundation for understanding the broader implications of including buildability factors in multi-criteria evaluation, particularly in relation to environmental impact. The following chapter will explore the meaning and relevance of these results in the context of theoretical frameworks and the objectives posed, as well as discuss the impact of the method used.

6

Discussion

In this chapter, the method implemented in the study and the received results are discussed. In addition, suggestions are presented for further studies.

6.1 Method discussion

The results of this study show that set-based design, when combined with a digital and automated workflow, has significant potential to support the evaluation of how various design parameters influence climate impact (CO_2 emissions), buildability and investment cost in the design of reinforced concrete girder bridges. The methodology enables structured exploration of a wide range of design alternatives, thereby facilitating informed decision-making based on project-specific objectives. The choice of an optimal design solution is thus no longer limited to a single evaluation criterion but can instead reflect a balanced consideration of multiple, and potentially conflicting objectives.

The methodology also demonstrates a potential to identify more efficient design alternatives. For example, as shown in the reference project, the SBD algorithm identified solutions with marginally improved buildability while achieving notably lower total costs. This highlights alternatives that may not have been apparent through conventional design methods. These findings are illustrated in Figure 5.12.

Furthermore, the developed algorithm is parametric and modular, enabling flexibility with respect to project-specific input conditions. For example, the span length of the girder bridge is defined as an input parameter and can easily be modified within the Python script to adapt the optimization to other bridge configurations. This flexibility increases the general applicability of the method across a broader range of projects.

However, a critical aspect when evaluating the set-based design method is the initial time investment required to develop the algorithm. The more advanced the design subject is, the more time is required to implement the design parameters in code. Additionally, each analysis and evaluation performed increases both the development time and the computational time when running the final script. Developing a sufficiently advanced algorithm requires a significant amount of work. However, when the algorithm is finalized, its flexibility and ability to provide relevant data, as a basis for decision-making, might save time in other processes. It would be interesting for future work to investigate set-based design among other design methods to further test its efficiency and compare what solutions they create given the same design problem.

In addition, the study and its method have several limitations. Some constraints were deliberately introduced to define the scope and maintain the feasibility of the study, such as simplifications in structural modeling and reinforcement design. Others may affect the precision and generalization of the results, particularly concerning the accu-

racy of the buildability and cost estimations. These limitations are elaborated on in the following sections.

6.1.1 Implications of excluding pre-stressing in the FE model

One of the simplifications made in this study was the decision to model the reference bridge using conventional reinforcement instead of post-tensioned pre-stressing. In the original reference project, the bridge was designed with post-tensioned pre-stressing and minimal tensile reinforcement, primarily to control surface cracking. For the purpose of this study, this was modified in the FE model, where the structure was considered to be reinforced without pre-stressing. This choice was made to simplify the modeling process.

As mentioned in Section 2.2.3, girder bridges of this span length, over 30 meters, are commonly pre-stressed to satisfy serviceability criteria, such as limiting deflection and controlling long-term deformations. While it is technically possible to design such structures using only conventional reinforcement, doing so generally offers less margin for fulfilling these requirements. Nevertheless, the modification was considered acceptable within the scope of this study, given that the developed algorithm is parametric and can be applied to various span lengths. In practice, the methodology may be more suitable for bridges with spans under 30 meters or for cases where reinforcement is deemed sufficient. Alternatively, future work could incorporate pre-stressing into the modeling process, which is feasible and would increase the accuracy and applicability of the approach. Although this simplification introduces certain limitations in terms of structural representation, it was judged to be sufficient for demonstrating the core functionality and adaptability of the proposed method.

6.1.2 Buildability considerations for I-shaped girders

The choice of production method has a direct impact on the assessment of the buildability for different girder shapes. In this study, both I-shaped and rectangular girders were assumed to be cast in situ. Prefabricated alternatives were excluded, primarily due to the logistical and economic challenges of transporting large concrete elements. Standard truck dimensions typically limit prefabricated components to a maximum length of approximately 12 meters. Beyond this, transportation costs increase significantly, making such solutions less feasible for longer-span bridges. As a result, in situ casting is more suitable for the span lengths of the reference project. However, for shorter-span bridges where transportation is less restrictive, prefabrication could offer substantial buildability benefits. In such cases, the difference in buildability between I-shaped and rectangular girders might diminish, particularly since prefabricated I-girders could also allow for better quality control in production, for example with respect to temperature and weather conditions. This suggests that while in situ casting was appropriate for the current study, conclusions regarding buildability may vary depending on the span length and the chosen production method.

The I-shaped girder design also introduces specific construction challenges that affect buildability and require careful consideration. The geometry of I-shaped girders makes them more sensitive to casting issues, such as poor compaction in narrow sections. As presented in Section 4.3, the inclinations of the bottom of the upper flange and the top of the lower flange were introduced to improve casting conditions, although

this adds slightly to the volume of concrete required. Despite these complexities, the optimization results show that I-shaped girders outperform rectangular alternatives in terms of material efficiency, environmental impact, and investment cost. However, their shape can introduce additional design demands. For example, the contrast in thickness between the web and flanges may increase the risk of thermal cracking, necessitating preventive design measures and additional calculations. Thus, while I-shaped girders offer significant advantages in optimized designs, their practical implementation may require mitigation strategies to address their inherent buildability challenges that are uncommon in current practice.

6.1.3 Assumptions and limitations in cost and buildability factors

How aspects of buildability are quantified, through factors or additional cost, directly affects the results of the buildability cost. In this study, most values used for buildability considerations were derived from previous research, where assumptions were informed by consultations with practicing engineers at established firms. Additionally, the estimate of extra labor time required for constructing I-shaped girders, compared to rectangular ones, was obtained through similar industry-informed assumptions developed specifically for this study. Although this lends some degree of credibility, these values cannot be considered universally reliable. For practical implementation of an SBD algorithm, company-specific data should be used, as assumptions can vary depending on the experience and methods of the contractor. Although these values are not based on scientific measurement, they reflect the kind of experience-based estimation commonly used in the industry for economic assessments. As such, despite inherent uncertainties, the buildability factors applied in this study are assumed to be sufficient to demonstrate the potential of the SBD methodology and to explore how buildability correlates with environmental impact and cost.

The assumed material and labor costs used in this study are subject to uncertainty since market prices change over time. For example, the cost values from Yavari et al. (2016) and Yavari et al. (2017) are approaching a decade old and probably no longer align with current market prices. However, since the study focuses on comparing alternatives rather than providing absolute cost estimates, the relative differences between material costs remain valuable for the analysis. Nonetheless, the use of updated and region-specific cost parameters is recommended for future applications or implementation in practice, to enhance the accuracy and applicability of the results.

The exclusion of formwork from the analysis introduces a limitation in assessing both buildability and cost. Formwork affects all three aspects: investment cost, environmental cost, and buildability cost, due to its addition of material and labor hours. Its complexity and volume would be influenced by the geometric characteristics of the structural elements. It is fair to assume that I-shaped girders would require significantly more intricate and labor-intensive formwork compared to rectangular girders, potentially influencing the buildability cost to a degree comparable to that of the girder shape factor applied in this study. Consequently, this simplification may have led to an underestimation of the buildability cost and investment costs across the design alternatives analyzed. However, the formwork was excluded from the scope of the thesis primarily due to its complexity and the time constraints. Future research is encouraged to address this gap and to integrate formwork estimation into comparative assessments, especially when evaluating design solutions that differ significantly in geometry or construction

complexity.

6.2 Discussion of results

When mapping out the probability density functions of the design spaces with respect to the different criteria, distributions are not consistent, but vary from mostly normal to multi-modal distributions, as seen in Figures 5.1-5.3. These distributions reflect the different cost definitions and are expected parts of the result. All cost definitions contain more than one function, contributing to the diverging distributions, but buildability models the extreme case with multiple prominent local maxima and minima. The larger range on the x-axis observed in the buildability plot compared to the other two is also a result of the criteria definition. Since the buildability cost is considered as an additional labor cost, apart from the entirely volume-dependent labor cost included in the investment cost, some options with a high level of buildability result in a very low buildability cost. With the lowest value in the range normalized to 1, the range then becomes larger than seen in the other two criteria.

The location of the reference project within the probability density distributions suggests that there is room for improvement when it comes to CO_2 emissions and investment cost, as there are many possible solutions with lower costs in these criteria. Interestingly, the reference bridge is fairly optimized when it comes to buildability, as only a small portion of solutions with lower buildability cost exist in the design space. This again emphasizes the importance of a multi-criteria evaluation, as a high performance in one criterion does not guarantee a good performance in the other two. The reference bridge being among the options with the lowest buildability cost is explained by the fact that it satisfies both of the key factors that were pointed out as contributors to improved buildability, namely a rectangular girder shape and low concrete class. Since relatively few combinations that use both of these two parameters exist within the design space, the set of alternatives considered more optimized on buildability than the reference project is small. This also underlines the overall priority within construction companies to find solutions with short construction time.

The compound effect of multiple functions that make up the buildability criterion affects the predictability of where a solution will fit on the distribution of the scatter plots. As seen in Figures 5.6 and 5.7, as opposed to Figure 5.5, the link between buildability and the two other criteria is much weaker than the correlation between investment cost and environmental cost. Hence, the final cost for the client of solutions with a high level of buildability can vary largely, making it an unfitting criterion to solely optimize for, as the financial aspect is the deciding factor for companies when going through the design process in a real scenario. These observations highlight the importance of considering all criteria jointly during decision-making, as optimizations in one parameter can significantly influence the others.

As the comparison of the total cost of a few bridges in Design Space D showed in Figure 5.12, the alternative with the lowest total cost and CO_2 emissions had a higher buildability cost than the others. A similar result was found by Bergenram and Ulander (2023), where the most geometrically optimized solution reduced emissions by 13.7%, but doubled the buildability cost. The results of this study are of a similar scale, where a reduction of 27.7% could be observed in environmental cost, while the buildability cost increased by 162.5% for the best performing I-profile alternative. Despite the two

studies analyzing different bridge types, these numbers suggest that the set-based design method has the potential to find bridge solutions with reduced climate impact, but that the level of buildability is largely affected in geometrically optimized designs.

Figure 5.12 also shows that the buildability cost does not represent a large part of the total cost, which means that the solution with the lowest environmental impact also results in the lowest total cost for the client. This does not make buildability irrelevant to study but is rather a question of where money is spent in a project. As environmental cost is not a commonly used tool in tendering processes today, the fact that there are solutions with a lower total cost than the reference, even without environmental cost accounted for, is of importance to the results. This means that the set-based design method used in this study has found solutions with lower climate impact, which was one of the objectives, but also provided alternatives relevant to the current tendering process structure.

Environmental sustainability is not yet a standardized cost factor in most infrastructure tendering processes. In fact, most public procurement still relies on either the Lowest Price or the Lowest Total Cost method, both of which prioritize financial efficiency over long-term environmental value. This is despite the development of strategic action plans such as the Roadmap for Fossil Free Competitiveness for the construction and civil engineering sector, which highlights the need for transformative changes in the industry, and places strong emphasis on the early stages of project development where design decisions can have the greatest impact on environmental outcomes while still maintaining cost efficiency.

To align tendering processes with evolving environmental priorities, systemic reforms are necessary, as presented in the road map. One major challenge lies in creating economic incentives for contractors to propose environmentally sound designs. Without financial benefits, sustainability considerations are unlikely to be prioritized in competitive bidding scenarios. This calls for a shift in procurement strategies in which the environmental impact is not treated as an externality but as an integral part of the evaluation of the project. One way to approach this is by incorporating climate cost in tendering processes, along with economic cost. In this context, the set-based design method presented offers valuable benefits. By improving the quality of information available early in the design phase, it enables more informed decisions and facilitates comparisons between economically optimal and environmentally sound design alternatives. This approach has potential as a decision support tool in negotiations during the tendering process, encouraging more sustainable infrastructure development.

6.3 Possible further studies

Apart from the possible areas of future work previously mentioned, this section provides additional research areas to investigate the field of set-based design within civil engineering.

Several interesting aspects for future research lie in expanding the scope of optimization parameters in this study. For instance, this study assumes a constant cross-section along the girder span, except for reinforcement curtailment. However, varying the height of the girders along the span to better align with the distribution of the bending moment, could reduce material usage without compromising structural performance. Moreover, investigating how this optimization would affect the relationship between material sav-

ings and buildability cost would be interesting. In addition, future research could investigate how different buildability criteria behave under varying input conditions. For example, changing the initial parameters that define Design Space B could shift which buildability factors dominate the decision-making process. A sensitivity analysis or parametric study across different project types and constraints would provide a broader understanding of how context influences buildability assessment in design automation. Another possible dimension to geometrical optimization is to introduce more girders or the addition of field support, thus also analyzing the bridge at a structural system level. This approach could be tested for different types of girder bridges or extended to other types of bridges to evaluate the generalization of the findings.

Another possible direction for future research could explore the implementation of an SBD algorithm for more complex bridge cross-sections, such as a box girder bridge. Due to time constraints, this study was limited to analyzing only two types of cross-sections of the girder bridge, and therefore, box girders were excluded. Box girders involve more complex geometries and a greater number of design parameters, which would increase the complexity of the optimization process. Nevertheless, they offer several advantages that make them highly relevant for further study. In addition to their favorable structural performance and torsional stiffness in long spans, box girders also show significant potential for material reduction. The study by Kettil (2023) provided estimated values that indicate that I-shaped and box girder bridges can achieve similar reductions in material use. Had box girders been included, the broader design space and increased complexity would likely have posed greater computational demands, but may also have revealed alternate material-efficient solutions. When environmental considerations are increasingly prioritized in bridge design, the efficient use of materials reinforces the relevance of box girders in future research. Although challenges such as inspection access in short-span applications remain, the broader advantages of box girder cross-sections make them a promising subject for further investigation.

To facilitate the practical application of this method in real-world projects, further studies are necessary. Applying the methodology to various case studies would demonstrate its robustness and adaptability and help identify the conditions under which it offers the most value. Moreover, since the approach enables exploration of design alternatives that may not be considered in traditional workflows, continued research could support its integration into the early design stages. This would increase both its usability and its acceptance in industry practice. Ultimately, by refining and validating this method in various contexts, the potential for design automation to support more sustainable and buildable bridge solutions can be more fully realized.

7

Conclusion

This study demonstrates that set-based design (SBD), when integrated with a digital and automated workflow, has the potential to support decision-making in the early-stage design of reinforced concrete girder bridges. The method facilitates systematic exploration of a broad design space, enabling the evaluation of how different design parameters affect climate impact (in terms of CO_2 emissions), buildability, and investment cost. For example, the study identified alternatives with rectangular girders with marginally lower buildability cost compared to the reference project, but notably reduced total cost. This evidences the strength of SBD in uncovering efficient, non-obvious design options by considering multiple, often conflicting, objectives simultaneously. Furthermore, the parametric and modular structure of the developed algorithm allows it to be adapted to different project conditions, such as varying span lengths or loading requirements. This adaptability increases the general applicability of the method, making it a promising tool for a broader use in infrastructure planning and sustainable bridge design.

The study investigated and implemented buildability aspects into the automated design of girder bridges. The results indicate that the shape of girder and the concrete class are the most influential factors affecting the cost in all criteria. The rectangular-shaped girders generally resulted in lower buildability costs, whereas I-profile girders are generally more favorable in terms of CO_2 emissions. Furthermore, concrete class C50/60 was associated with significantly higher buildability and environmental costs than the lower-strength classes C35/45 and C32/40. Although, the results also show the importance of employing a multi-criteria evaluation framework, as optimization based on a single criterion does not necessarily lead to holistic optimal solutions.

An additional observation of this study is that material consumption can have a greater influence on total cost than buildability. When comparing the alternative with the lowest cost from each girder category, the I-profile alternative exhibited the lowest total cost, despite incurring a higher buildability cost than the rectangular one. This suggests that material efficient cross-section designs can yield substantial overall cost benefits than optimizing solely for buildability. However, the potential production challenges associated with I-shaped concrete girders make for uncertainties in its practical buildability. This introduces some uncertainty into the implemented buildability costs and suggests that actual implementation could result in higher costs than those estimated in this study. Further research is therefore recommended to examine material-efficient configurations such as I-shaped girders in more depth, particularly with respect to production feasibility, to fully understand their potential for reducing both material use and total cost.

The findings of this study also highlight the potential of SBD to serve as a decision-support tool in procurement and tendering processes. As climate impact becomes an

increasingly relevant factor in infrastructure planning, the automated integration of environmental evaluation within the SBD framework enables designers to compare environmentally sound alternatives with economically optimal ones at an early stage. This contributes to greater transparency and enables more informed negotiations during tendering by clearly articulating the trade-offs between key criteria such as cost, buildability, and environmental performance. Ultimately, the study demonstrates that a set-based design methodology can facilitate a more holistic approach to early-phase bridge design by identifying optimal compromises, enhancing the quality of available information, and enabling more sustainable and cost-efficient infrastructure development.

References

Al-Emrani, M., Engström, B., Johansson, M., & Johansson, P. (2019). *Bärande konstruktioner: Del 1* (Vol. ACE 2019:2). Report\Department of Architecture; Civil Engineering, Chalmers University of Technology.

Ålenius, M. (2003). *Finite Element Modelling of Composite Bridge Stability*, KTH Royal Institute of Technology, Master's Thesis. https://www.mech.kth.se/~pelleth/MScThesisMartinWeb.pdf

Bergenram, F., & Ulander, S. (2023). *Set-Based Multi-Criteria Optimization of Slab Frame Bridges: A Study on the Implementation of a Set-Based Multi-Criteria Optimization Algorithm on Slab Frame Bridges, considering Investment Cost, Environmental Impact and Buildability*, Chalmers University of Technology, Master's Thesis. http://hdl.handle.net/20.500.12380/306810

Bergenram, F., Ulander, S., Rempling, R., Kjellgren, A., & Broo, H. (2024). Parametric Optimization of Slab Frame Bridges Considering Investment Cost, Environmental Impact and Buildability. *Procedia Computer Science*, *239*, 193–200. https://doi.org/10.1016/J.PROCS.2024.06.162

Björnsson, I., Kamrad, T., Lundstedt, K., Thelandersson, S., Lövquist, A., & Gustavsson, S. (2025, February). *Resursslöseri i anläggningsbyggandet?: Vad kan vi lära av 50 års utveckling?* Div. of Structural Engineering, Lund University. https://portal.research.lu.se/sv/publications/resurssl%C3%B6seri-i-anl%C3%A4ggningsbyggandet-vad-kan-vi-l%C3%A4ra-av-50-%C3%A5rs-ut

Bragança, L., Vieira, S. M., & Andrade, J. B. (2014). Early stage design decisions: The way to achieve sustainable buildings at lower costs. *The Scientific World Journal*, *2014*. https://doi.org/10.1155/2014/365364

Concrete Bridge Development Group. (n.d.). Types of Concrete Bridges. https://www.cbdg.org.uk/types-of-bridges.asp

El Mourabit, S. (2016). Optimization of Concrete Beam Bridges : Development of Software for Design Automation and Cost Optimization. https://www.diva-portal.org/smash/record.jsf?pid=diva2%3A945092&dswid=-1894

Eriksson, T. A. S. (2013). *Organising the Early Design Phase in a Large Infrastructure Project (Licentiate Thesis)* [Doctoral dissertation, Chalmers University of Technology].

Fernández, S. L., & Ramos, D. T. (2014). *Applicability of Set-Based Design on Structural Engineering*, Chalmers University of Technology, Master's Thesis. https://www.semanticscholar.org/paper/Applicability-of-Set-Based-Design-on-Structural-Fern%C3%A1ndez-Ramos/4588164f8090bf58ab2621032a4fb6162879e8e3#citing-papers

Finnveden, G., Håkansson, C., & Noring, M. (2013). A new set of valuation factors for LCA and LCC based on damage costs: Ecovalue 2012. *Perspectives on managing life cycles: Proceedings of the 6th International Conference on Life Cycle Management*, 197–200. https://kth.diva-portal.org/smash/record.jsf?pid=diva2%3A739101&dswid=9907

Fossilfritt Sverige. (2024, February). *Färdplan för fossilfri konkurrenskraft: Bygg- och anläggningssektorn* (tech. rep.). https://fossilfrittsverige.se/roadmap/bygg-och-anlaggningssektorn/

Hammervold, J., Reenaas, M., & Brattebø, H. (2013). Environmental life cycle assessment of bridges. *Journal of Bridge Engineering*, *18*(2), 153–161. https://doi.org/10.1061/(ASCE)BE.1943-5592.0000328

Hansson, L., & Tacking, N. (2024). *Set-Based Design: A Method for Improving Requirement Definition in the Bridge Procurement Process: How Set-Based Design Can Manage Uncertainty in the Preliminary Design Phase and Procurement of Frame Bridges*, Chalmers University of Technology, Master's Thesis. https://odr.chalmers.se/items/c0775b01-9e94-4be3-b827-d3c49f3310ea

Hernandez, C. R. B. (2006). Thinking parametric design: introducing parametric Gaudi. *Design Studies*, *27*(3), 309–324. https://doi.org/10.1016/J.DESTUD.2005.11.006

Kettil, P. (2023, March). *Klimatoptimerade betongbroar – Geometri och material* (tech. rep.). SBUF. Göteborg. https://vpp.sbuf.se/Public/Documents/ProjectDocuments/a1fee162-2913-44a0-b043-5257800a972a/FinalReport/SBUF%2014143%20Slutrapport%20Klimatoptimerade%20betongbroar%20geometri%20och%20material.pdf

Khouri Chalouhi, E. (2019, March). *Optimal design solutions of concrete bridges considering environmental impact and investment cost (Licentiate Thesis)* [Doctoral dissertation, KTH Royal Institute of Technology].

Khouri Chalouhi, E., Pacoste, C., & Karoumi, R. (2019). Topological and Size Optimization of RC Beam Bridges: An Automated Design Approach for Cost Effective and Environmental Friendly Solutions. *Nordic Concrete Research*, *61*(2), 53–78. https://doi.org/10.2478/NCR-2019-0017

Kohler, N., & Moffatt, S. (2003). Life-cycle analysis of the built environment. *UNEP Industry and Environment*, 17–21. https://www.researchgate.net/publication/279711810_Life-cycle_analysis_of_the_built_environment

Kwon, K., Kim, D., & Kim, S. (2021). Cutting waste minimization of rebar for sustainable structural work: A systematic literature review. *Sustainability*, *13*(11), 5929. https://doi.org/10.3390/SU13115929

Lea, F. M., & Mason, T. O. (2025, February). Cement. https://academic-eb-com.eu1.proxy.openathens.net/levels/collegiate/article/cement/108319

Lee, J. H., & Ostwald, M. J. (2020). Creative Decision-Making Processes in Parametric Design. *Buildings 2020, Vol. 10, Page 242*, *10*(12), 242. https://doi.org/10.3390/BUILDINGS10120242

Lu, W., Liang, C., Fung, A., & Rowlinson, S. (2014). Demystifying the Time-Effort Distribution Curves in Construction Projects: A BIM and non-BIM Comparison, 329–338. https://doi.org/10.1061/9780784413517.034

Mathern, A., Rempling, R., Ramos, D. T., & Luis Fernández, S. (2018). Applying a set-based parametric design method to structural design of bridges. https://research.chalmers.se/publication/508228/file/508228_Fulltext.pdf

Mathern, A., Steinholtz, O. S., Sjöberg, A., Önnheim, M., Ek, K., Rempling, R., Gustavsson, E., & Jirstrand, M. (2021). Multi-objective constrained Bayesian optimization for structural design. *Structural and Multidisciplinary Optimization*, *63*(2), 689–701. https://doi.org/10.1007/S00158-020-02720-2/TABLES/7

Miliutenko, S. (2022, April). *Klimatkalkyl - Infrastrukturhållningens energianvändning och klimatpåverkan i ett livscykelperspektiv* (tech. rep.). Trafikverket. https://www.trafikverket.se/klimatkalkyl

Nahm, Y. E., & Ishikawa, H. (2005). Novel space-based design methodology for preliminary engineering design. *International Journal of Advanced Manufacturing Technology*, *28*(11-12), 1056–1070. https://doi.org/10.1007/S00170-004-2463-2/METRICS

Niveditha, M., Manjunath, Y. M., & Prasanna, S. H. (2020). Ferrock: A carbon negative sustainable concrete. *International Journal of Sustainable Construction Engineering and Technology*, *11*(4), 90–98. https://doi.org/10.30880/IJSCET.2021.11.04.008

Osuizugbo, I. C., Okolie, K. C., Oshodi, O. S., & Oyeyipo, O. O. (2023). Buildability in the construction industry: a systematic review. *Construction Innovation*, *23*(5), 1300–1322. https://doi.org/10.1108/CI-05-2022-0112/FULL/PDF

Parrish, K., Wong, J. M., Tommelein, I. D., & Stojadinovic, B. (2007). Exploration of set-based design for reinforced concrete structures. *Lean Construction: A New Paradigm for Managing Capital Projects - 15th IGLC Conference*, 213–222. https://asu.elsevierpure.com/en/publications/exploration-of-set-based-design-for-reinforced-concrete-structure

Purnell, P. (2012). Material nature versus structural nurture: The embodied carbon of fundamental structural elements. *Environmental Science and Technology*, *46*(1), 454–461. https://doi.org/10.1021/ES202190R/SUPPL{_}FILE/ES202190R{_}SI{_}002.PDF

Purnell, P. (2013). The carbon footprint of reinforced concrete. *Advances in Cement Research*, *25*(6), 362–368. https://doi.org/10.1680/ADCR.13.00013

Rempling, R., Mathern, A., Tarazona Ramos, D., & Luis Fernández, S. (2019). Automatic structural design by a set-based parametric design method. *Automation in Construction*, *108*, 102936. https://doi.org/10.1016/J.AUTCON.2019.102936

Sheng, K., Woods, J. E., Bentz, E., & Hoult, N. A. (2024). Assessing embodied carbon for reinforced concrete structures in Canada. *Canadian Journal of Civil Engineering*, *51*(8), 829–840. https://doi.org/10.1139/CJCE-2023-0345/ASSET/IMAGES/CJCE-2023-0345{_}TAB4.GIF

SIMULA. (2006, March). ABACUS Version 6.6 Documentation. https://classes.engineering.wustl.edu/2009/spring/mase5513/abaqus/docs/v6.6/books/usb/default.htm?startat=pt06ch23s03ael13.html

Swedish Institute for Standards. (2008, November). *Eurocode 2: Design of concrete structures – Part 1-1: General rules and rules for buildings* (1st ed.). SS-EN 1992-1-1:2005.

Swedish Institute for Standards. (2010, December). *Eurocode – Basis of structural design* (1st ed.). SS-EN 1990.

Swedish Institute for Standards. (2011, May). *Eurocode 1: Actions on structures – Part 2: Traffic loads on bridges*. SS-EN 1991-2.

Trafikverket. (2022). *Proposal national plan for transport infrastructure 2022-2033 - Summary* (tech. rep.). https://bransch.trafikverket.se/en/startpage/planning/long-term-infrastructure-planning/

Trafikverket. (2024, July). KRAV TRVINFRA-00227 (version 5.0): Bro och brolikknande konstruktion Byggande.

Transportstyrelsen. (2018). TSFS 2018:57: Transportstyrelsens föreskrifter och allmänna råd om tillämpning av eurokoder.

Uppenberg, S., Ekström, D., Liljenroth, U., & Al-Ayish, N. (2017, May). *Klimatoptimerat byggande av betongbroar: Råd och vägledning* (tech. rep.). SBUF. https://www.diva-portal.org/smash/record.jsf?pid=diva2%3A1747214&dswid=-1939

Vägverket. (2004, June). *Bro 2004* (2004:56).

Wimalaratne, P. L., Kulathunga, U., & Gajendran, T. (2021). Comparison between the terms constructability and buildability: A systematic literature review. *World Construction Symposium*, 196–207. https://doi.org/10.31705/WCS.2021.17

Yavari, M. S. (2017). *Slab Frame Bridges: Structural Optimization Considering Investment Cost and Environmental Impacts (Licentiate Thesis)* [Doctoral dissertation, KTH Royal Institute of Technology]. https://kth.diva-portal.org/smash/record.jsf?pid=diva2%3A1079393&dswid=-2106

Yavari, M. S., Du, G., Pacoste, C., & Karoumi, R. (2017). Environmental Impact Optimization of Reinforced Concrete Slab Frame Bridges. *Journal of Civil Engineering and Architecture*, *11*, 313–324. https://doi.org/10.17265/1934-7359/2016.04.001

Yavari, M. S., Pacoste, C., & Karoumi, R. (2016). Structural Optimization of Concrete Slab Frame Bridges Considering Investment Cost. *Journal of Civil Engineering and Architecture*, *10*, 982–994. https://doi.org/10.17265/1934-7359/2016.09.002

A

Software

A.1 BRIGADE/Plus and Abaqus

BRIGADE/Plus is a comprehensive software tool intended for the analysis and design of bridges and civil structures. It offers a user interface that integrates the modeling, analysis, and visualization of results. The software includes predefined loads, vehicles, and load combinations in accordance with various design codes, including the Eurocodes. The results can be visualized in 3D plots and 2D graphs, and the integrated report generator facilitates the creation of input and result reports. (technia hemsida)

One of the main features of BRIGADE/Plus is its integration with the Abaqus Finite Element Analysis (FEA) solver from SIMULIA. Abaqus is a powerful software suite for finite element analysis and computer-aided engineering, widely used for modeling and analyzing mechanical components and assemblies. The integration of Abaqus solver technology within BRIGADE/Plus allows for advanced analysis procedures, including static, dynamic, and coupled analyses. This combination enables users to perform detailed structural analyses of bridges and civil structures, taking into account complex factors such as moving loads, prestressing, and non-linear material behavior. The synergy between BRIGADE/Plus and Abaqus enhances the overall capabilities of the software, making it a robust tool for engineers and researchers in the field of structural engineering (Ålenius, 2003)

Table A.1: Notations in BRIGADE/Plus (SIMULA, 2006)

Notation	Description
U3	Deflection in the global 3-direction
SM1	Bending moment force per unit width about local 1-axis
SF2	Transverse shear force in the local 2-direction

B

Verification of FE Model

To validate the FE model of the reference project, it was compared to the results from the calculation report made of Skanska. In addition, hand calculations were made to verify and comply with the BRIGADE results. Details of the model are presented in Table B.1.

Table B.1: Elements in the FE model in BRIGADE/Plus.

Element	Element type	Amount
Main beam	Beam	2
Bridge deck	Shell	1
Edge beam	Beam	2
End cross beam	Beam	2
Middle cross beam	Beam	1

B.1 Self-weight

The expected reaction force and the maximum deflection, bending moment, and shear forces from the application of the self-weight load were calculated analytically and compared with the BRIGADE results; see Tables B.2 and B.3. The density ρ of reinforced concrete was assumed to be 25 kN/m^3 (Trafikverket, 2024).

In the calculations for the self-weight G [N], equation B.1 was used.

$$G = b \cdot h \cdot l \cdot \rho \tag{B.1}$$

where b, h and l is respectively the width, height and length of the bridge component.

Table B.2: Verification of reaction force.

Bridge component	Self-weight	
Slab	$0.3 * 9 * 25 = 67.5kN/m$	$67.5 * 35.5m = 2396.25kN$
Main beam	$1.4 * 1.2 * 25 * 2 = 84kN/m$	$84 * 35.5m = 2982kN$
Edge beam	$0.24 * 0.4 * 25 * 2 = 8.4kN/m$	$8.4 * 35.5m = 298.2kN$
End cross beam		$1.4 * 1.0 * 3.45 * 2 * 25 = 241.5kN$
Middle cross beam		$0.9 * 0.5 * 3.45 * 25 = 38.8kN$
	Total:	**5956.75 kN**
	Total reaction force from BRIGADE:	$1.490 * 10^6 * 4 =$ **5960 kN**

OK!

For deflection, the self-weight, g [N/m], is seen as a distributed load. The maximum shear force is estimated to be equal to the total self-weight distributed between the four support points.

Table B.3: Verification of self-weight modeling.

Parameter	Equation	Analytical result	BRIGADE result	Difference
δ_g	$\frac{5gL^4}{384*EI}$	62.6 mm	59.7 mm	5%
M_g (one beam)	$\frac{gL^2}{8*2}$	12.595 MNm	12.6 MNm	0%
V_g (one bean)	$G_{tot}/4$	1489 kN	1420 kN	5%

where L is the span length, EI is the stiffness of the cross-section, and G_{tot} is the total self-weight [kN]. The maximum moment is expected in the mid-span, were as the maximum shear force is expected near the supports.

B.2 Traffic load

The expected reaction force $R_{traffic}$ and maximum deflection $\delta_{traffic}$, bending moment $M_{traffic}$, and shear force $V_{traffic}$ from the application of the traffic load were calculated analytically and compared with the BRIGADE results; see Table B.4.

As mentioned in Section 3.2, the traffic load was applied according to the Bro 2004 regulation, resulting in a combination of distributed loads and point loads (axle loads) to simulated traffic, similar to the concept in LM1 in the current regulations. To get the maximum reaction force, two axle loads (P_1, P_2) and the distributed load ($q_{traffic}$) are added together.

Table B.4: Verification of traffic load application.

Parameter	Equation	Analytical result	BRIGADE result	Difference
$R_{traffic}$	$P_1 + P_2 + q_{traffic} \cdot L$	2007 kN	1999 kN	0.4%
$\delta_{traffic}$	$(P_1 + P_2) \cdot \frac{L^3}{48EI} + \frac{5q_{traffic}L^4}{384*EI}$	29.1 mm	29.4 mm	1.2%
$M_{traffic}$	$(P_1 + \frac{P_2}{2}) \cdot \frac{L}{2 \cdot 2} + \frac{q_{traffic}L^2}{8}$	10.02 MNm	9.30 MNm	7.8%
$V_{traffic}$	$P_1 + \frac{P_2}{2} + q_{traffic} \cdot L/2$	1213 kN	1179 kN	2.9%

C

Loads

This chapter describes the loads applied in the structural verification and how they were calculated according to standards.

C.1 Permanent loads

The concrete elements of the bridge were calculated with a density of 25 kN/m^3 and the pavement with 23 kN/m^3 (Trafikverket, 2024).

C.2 Variable loads

The traffic loads were applied according to LM1 in Eurocode ss-EN 1991-2 (Swedish Institute for Standards, 2011). The 9 m wide bridge deck gave three lanes, in which axle loads and distributed loads were implemented conforming to Figure C.1. The characteristic load values, including dynamic factor, were taken from Table C.1.

Table C.1: Load Model 1: Characteristic Values (SS-EN 1991-2 4.3.2 (4.2)).

Location	**Tandem system**	**Distributed load**
	Axle Load Q_k (kN)	**q_k (or q_{rk}) (kN/m^2)**
Lane 1	300	9
Lane 2	200	2.5
Lane 3	100	2.5
Other Lanes	0	2.5
Remaining area (q_{rk})	0	2.5

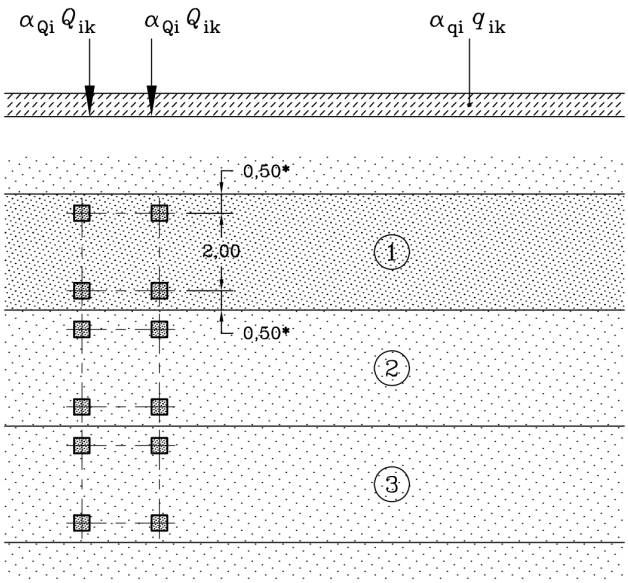

Figure C.1: LM1 application in lanes.

For bridges longer than 10 m, the tandem system load can be simplified to a concentrated force according to SS-EN 1991-2 4.3.2 (6)b. This means a force of 600, 400 and 200 kN for each lane, multiplied with an adjustment factor α. The adjustment factors are given in the national amendments, TSFS 2018:57, 4.3.3(4), viewed in Table C.2.

Table C.2: Adjustment factors α (Transportstyrelsen, 2018).

Adjustment factor	Value
α_{Q1}	0,9
α_{Q2}	0,9
α_{Q3}	0
α_{q1}	0,8
α_{qi}	$1,0$ for $i > 1$
α_{qr}	1,0

With i refering to the lane number and r the remaining areas.

The braking force is calculated according to SS-EN-1991-2 4.4.1(4.6), but limited to 500 kN in TSFS 2018:57. The equation is as follows:

$$Q_{1k} = 0.6\alpha_{Q1}(2Q_{1k}) + 0.10\alpha_{q1}q_{1k}W/L$$

The side forces is set to 25% of the braking force, according to SS-EN 1991-2 4.4.2 (4) and is considered simultaneously as the braking force at the upper surface of the pavement.

D

Verification of Resistance

D.1 Serviceability limit state

SLS verification was performed with regards to vertical deflection. The deflection, δ, given by the FEM model during the frequent load model was compared with the demand according to TRVINFRA-00227 (7.2.1.1.4.2.2) (Trafikverket, 2024), presented in equation (D.1).

$$\delta < L/400 \tag{D.1}$$

D.2 Ultimate limit state

This section presents the verifications of the resisting bending moment and shear in ULS.

D.2.1 Bending moment resistance

The calculation procedure for the bending moment resistance was performed according to (Al-Emrani et al., 2019). The cross section is assumed to have only tensile reinforcement; the concrete can carry all compression.

Geometry

b	Main beam width [mm]
h	Main beam height [mm]
ϕ	Diameter of reinforcement [mm]
d_i	Distance between top cross-section edge to center of reinforcement layer i [m]
x	Height of compression zone [m]
$\alpha = 0.8$	Stress block factor for simplified rectangular stress block [-]
$\beta = 0.4$	Simplified stress block factor for compressive force resultant position [-]

Material

$E_s = 200 \cdot 10^9$	Elastic modulus of reinforcement steel [Pa]
ϵ_{syd}	Design yielding strain of reinforcement [-]

$f_{yk} = 500 \cdot 10^6$	Characteristic yielding strength of reinforcement [Pa]
$f_{yd} = f_{yk}/1.15$	Design yielding strength of reinforcement [Pa]
f_{ck}	Characteristic compressive strength of concrete [Pa]
$f_{cd} = f_{ck}/1.5$	Design compressive strength of concrete [Pa]
$\epsilon_{cu} = 3.5 \cdot 10^{-3}$	Ultimate strain of concrete [-]
	(SS-EN 1992-1-1:2005, Table 3.1)

Sectional forces

M_{Ed}	Design bending moment [Nm]

Necessary amount of tensile reinforcement

The necessary reinforcement area can be approximated according to (Al-Emrani et al., 2019)[Section B4.3.2]:

$A_s \approx \frac{M_{Ed}}{f_{yd} \cdot 0.9 \cdot d}$

A_s was used as the basis for the generation of rebar layout, see Section 4.1.1. In accordance with the design of the reference project, c_{nom} was set to 40 mm.

Design bending moment resistance

The design bending moment resistance of the cross-section design with the generated rebar layout was then calculated using equilibrium, the deformation condition and the constitutive relationship of steel (Al-Emrani et al., 2019, Section B5.2.2). And specifically for the bridges with I-beam cross-section, the guide in Section B5.3.2 (Al-Emrani et al., 2019) was followed.

The height of the compression zone can be determined on the equilibrium of the horizontal cross-sectional forces, as in equation (D.2).

$$\rightarrow: \alpha \cdot f_{cd} \cdot b \cdot x = \sum(\sigma_{si} \cdot A_{si}) \tag{D.2}$$

The stress of each reinforcement layer can be expressed by equation (D.3), based on the idealized stress-strain relation with horizontal branch.

$$\sigma_{si} = \begin{cases} E_s \cdot \epsilon_s, & \epsilon_s < \epsilon_{syd} \\ f_{yd} & \epsilon_s > \epsilon_{syd} \end{cases} \tag{D.3}$$

The steel strain of each rebar layer can be expressed in terms of the ultimate compressive strain of concrete, see equation (D.4), assuming a linear strain distribution and full interaction between concrete and reinforcement.

$$\epsilon_{si} = \frac{d_i - x}{x} \cdot \epsilon_{cu} \tag{D.4}$$

The bending moment resistance was calculated by moment equilibrium around the top reinforcement layer (with the internal lever arm as z_{top}) according to equation (D.5).

$$M_{Rd} = \sum(\sigma_{si} \cdot A_{si} \cdot (z_i - z_{top})) + \alpha \cdot f_{cd} \cdot b \cdot x \cdot z_{top} \tag{D.5}$$

where $z_i = d_i - \beta \cdot x$.

D.2.2 Shear resistance

The resistance and design of shear reinforcement was performed according to SS-EN 1992-1-1:2005 (Swedish Institute for Standards, 2008). The need for shear reinforcement was checked according to SS-EN 1992-1-1:2005 (6.2.2), that is, the shear resistance of the concrete cross-section without shear reinforcement. The distance d was set to be between the top edge of the cross-section and the gravity center of the tensile reinforcement.

In regions where the applied shear force is greater than the design shear resistance of the concrete, $V_{Ed} > V_{Rd,c}$, shear reinforcement should be added to accommodate the need, so that $V_{Ed} < V_{Rd}$. The calculation procedure followed the equations in SS-EN 1992-1-1:2005 (6.2.3) and (9.2.2). The following assumptions were made:

- The shear reinforcement was assumed to be vertical.
- The angle θ between the concrete compression strut and the beam axis perpendicular to the shear force was set to 21.8°, so that $cot(\theta) = 2.5$.
- In accordance with the design of the reference project, the diameter of the shear reinforcement was chosen as $\phi 20$.
- The length of a shear reinforcement stirrup $l_{stirrup}$ was calculated as the circumference of a square inside the web with a distance to the edge of $40mm(c_{nom}) + \phi_{shear}/2$, plus $2 \cdot 10\phi$ for anchorage length.
- The spacing s between stirrups was chosen so that $V_{Rd,s}/s \geq V_{Ed}$.
- The design yield strength was limited to $0.8f_{ywd}$ and the reduction factor ν_1 was set $= 0.6$.

The volume of shear reinforcement was then calculated with equation (D.6).

$$V_{s,shear} = A_{sw} \cdot l_{stirrup} \cdot n \tag{D.6}$$

where $A_{sw} =$ cross-section area of one stirrup, $l_{stirrup} =$ length of one stirrup, and $n =$ number of stirrups.

E

Criteria Calculation

In order to compare different bridge design solutions, the environmental impact cost, investment cost and buildability cost was calculated.

E.1 Environmental impact cost

The environmental impact cost of the concrete and reinforcement was calculated by equations (E.1) and (E.2). The environmental impact unit costs and monetary weighting factor are presented in Table E.1.

$$EnvCost_{conc} = EnvCost_{unit,conc} \cdot V_c \cdot \beta_{monetary} \tag{E.1}$$

$$EnvCost_{reinf} = EnvCost_{unit,reinf} \cdot (V_s + V_{s,shear}) \cdot \rho_s \cdot \beta_{monetary} \tag{E.2}$$

where:

- $V_c =$ volume of concrete,
- $V_s =$ volume of tensile reinforcement, including anchorage length according to Section 4.3,
- $V_{s,shear} =$ volume of shear reinforcement, anchorage length included according to Section D.2.2, and
- $\rho_s = 7800$ kg/m^3 = density of reinforcing steel.

The total environmental impact cost was then calculated according to equation (E.3).

$$EnvCost = EnvCost_{conc} + EnvCost_{reinf} \tag{E.3}$$

Table E.1: Environmental impact unit costs and monetary value factor, according to (Yavari et al., 2017).

Concrete class	**Notation**	**Unit impact [$kg \cdot CO_2eq/m^3$]**
C32/40	$EnvCost_{unit,conc}$	344.505
C35/45		352.694
C50/60		383.748
Reinforcement	**Notation**	**Unit impact [$kg \cdot CO_2eq/kg$]**
B500B	$EnvCost_{unit,reinf}$	$2387.489 \cdot 10^{-3}$
Monetary weighting factor	**Notation**	**Price factor [$SEK/kgCO_2eq$]**
Ecovalue12	$\beta_{monetary}$	2.85

E.2 Investment cost

The investment cost was considered to include both the cost of material and labor, see equation (E.4).

$$InvestmentCost = MaterialCost + LaborCost \tag{E.4}$$

The total cost of material was calculated as the sum of the concrete and reinforcement material for the amount needed for each bridge solution, see equation (E.5). Unit material prices are presented in Table E.2.

$$MaterialCost = MaterialCost_{unit,conc} \cdot V_c + MaterialCost_{unit,reinf} \cdot (V_s + V_{s,shear}) \tag{E.5}$$

Table E.2: Unit material prices according to (Yavari et al., 2016).

Material	**Notation**	**Cost**
Concrete C32/40	$MaterialCost_{unit,conc}$	1700 SEK/m^3
Concrete C35/45		1800 SEK/m^3
Concrete C50/60		2000 SEK/m^3
Reinforcement	$MaterialCost_{unit,reinf}$	9 SEK/kg

The total labor cost was calculated as the sum of the labor cost of the concrete and reinforcement for the amount of material needed for each bridge solution, see equation (E.6). Unit labor prices are presented in Table E.3.

$$LaborCost = LaborCost_{conc} \cdot V_c + LaborCost_{reinf} \cdot (V_s + V_{s,shear}) \cdot \rho_s \tag{E.6}$$

Table E.3: Unit labor prices for RC beam bridges according to (El Mourabit, 2016).

Labor	Notation	Cost
Concrete super structure	$LaborCost_{unit,conc}$	750 SEK/m^3
Reinforcement in super structure	$LaborCost_{unit,reinf}$	15 SEK/kg

E.3 Buildability cost

How the buildability cost is calculated in more detail is described by equations (E.7)-(E.10) based on the chosen buildability criteria, mentioned in Section 4.3. The buildability factors and the additional cost due to buildability are presented in Table E.4.

Table E.4: Considered buildability aspects and their buildability factors and additional cost due to buildability.

Rebar diameter	**Notation**	**Price factor [-]**
ϕ16	α_ϕ	0.25
ϕ20		0.14
ϕ25		0
Slenderness of cross-section	**Notation**	**Price factor [-]**
$t < 400$ mm	α_{sl}	0.2
400 mm $< t <$ 600 mm		0.1
$t > 600$ mm		0
Shape of girder	**Notation**	**Price factor [-]**
Rectangular	α_{shape}	0
I-shape		0.5
Shear reinforcement	**Notation**	**Price factor [-]**
Stirrups are not needed	α_{shear}	0
Stirrups are used		0.56
Concrete class	**Notation**	**Unit price [SEK/m^3]**
$f_{ck} \geq 50$ MPa	$BuildCost_{C50/60}$	200
$f_{ck} < 50$ MPa		0

Buildability cost associated with bending reinforcement

The size of the reinforcement diameter, the slenderness of the cross-section, and the shape of the girder are all criteria that affect the buildability cost associated with the reinforcement, and it can be expressed by equation (E.7).

$$BuildCost_{reinf} = (\alpha_\phi + \alpha_{sl} + \alpha_{shape}) \cdot V_s \cdot \rho_s \cdot LaborCost_{unit,reinf} \tag{E.7}$$

Buildability cost due to the use of shear reinforcement

The addition and amount of shear reinforcement is assumed to result in a buildability cost, expressed by equation (E.8).

$$BuildCost_{shear,reinf} = \alpha_{shear} \cdot V_{s,shear} \cdot \rho_s \cdot LaborCost_{unit,reinf} \tag{E.8}$$

Buildability cost associated with concrete

An additional building cost due to longer labor time for concrete class C50/60 was implemented by equation (E.9).

$$BuildCost_{conc,class} = BuildCost_{C50/60} * V_c \tag{E.9}$$

The total buildability cost

The objective function related to the buildability criteria is a summation of these three previous equations, and can be expressed as in equation (E.10).

$$BuildCost = BuildCost_{reinf} + BuildCost_{shear,reinf} + BuildCost_{conc,class} \tag{E.10}$$

DEPARTMENT OF ARCHITECTURE AND
CIVIL ENGINEERING
CHALMERS UNIVERSITY OF TECHNOLOGY
Gothenburg, Sweden 2025
www.chalmers.se

CHALMERS
UNIVERSITY OF TECHNOLOGY